DOI:10.14753/SE.2025.3157

PREDICTION OF IMMUNE CHECKPOINT INHIBITOR THERAPY IN UROTHELIAL CARCINOMA: INTEGRATED ANALYSIS OF MOLECULAR PATTERNS AND CLINICAL FACTORS

PhD thesis

Melinda Rita Hermann-Váradi

Semmelweis University Doctoral School

Surgical Medicine Division

Supervisor: Tibor Szarvas, D.Sc.

Official reviewers: Csaba Bödör, D.Sc.

Tamás Beöthe, MD, Ph.D.

Head of the Complex Examination Committee:

Ilona Kovalszky, MD, D.Sc.

Members of the Complex Examination Committee:

Gábor Lotz, MD, D.Sc.
Tibor Füle, Ph.D.

Budapest
2025

DOI:10.14753/SE.2025.3157

Table of Contents

DOI:10.14753/SE.2025.3157

DOI:10.14753/SE.2025.3157

List of Abbreviations

1L – First-line

2L – Second-line

AC – Adjuvant chemotherapy

Ba/SCC-like – Basal/Squamous cell carcinoma-like molecular subtype

Ba/Sq – Basal/Squamous molecular subtype

BC – Bladder cancer

CI – Confidence interval

CIS – *In situ carcinoma*

CR – Complete response (remission)

CRP – C-reactive protein

CTLA-4 – Cytotoxic T-Lymphocyte Antigen-4

DCR – Disease control rate

DOR – Duration of response

ECOG PS– Eastern Cooperative Oncology Group performance status

eGFR – Estimated glomerular filtration rate

ELISA – Enzyme-Linked Immunosorbent Assay

FDA – Food and Drug Administration

FDR – False discovery rate

FFPE – Formalin-fixed, paraffin-embedded

GU – Genomically unstable molecular subtype

IC – Induction chemotherapy

ICI – Immune checkpoint inhibitor

IHC – Immunohistochemistry

LDH – Lactate dehydrogenase

LN – Lymph node

Lum – Luminal molecular subtype

LumI – Luminal-infiltrated molecular subtype

LumNS – Luminal non specified molecular subtype

LumP – Luminal-papillary molecular subtype

LumU– Luminal unstable molecular subtype

MDA – MD Anderson Cancer Center

Mes-like – Mesenchymal-like molecular subtype

MIBC – Muscle-invasive bladder cancer

mUC – metastatic urothelial carcinoma

NAC – Neoadjuvant chemotherapy

Ne – Neuronal molecular subtype

Ne-like – Neuroendocrine-like molecular subtype

NLR – Neutrophil-lymphocyte ratio

NMIBC – Non-muscle invasive bladder cancer

OS – Overall survival

ORR – Overall response rate

PC – Palliative chemotherapy

PD – Progressive disease

PD-1 – Programmed Death-1

PD-L1 – Programmed Death-Ligand1

PFS – Progression-free survival

PR – Partial response

RCE – Radical cystectomy

RCT – Radio chemotherapy

RNU – Radical nephroureterectomy

RT – Radiotherapy

Sc/Ne-like – Small-cell/Neuroendocrine-like molecular subtype

SD – Stable disease

TCGA – The Cancer Genome Atlas

TMB – Tumor mutational burden

UC – Urothelial carcinoma

Uro-like – Urothelial-like molecular subtype

UTUC: – Upper tract urothelial carcinoma

DOI:10.14753/SE.2025.3157

1. Introduction

Urothelial carcinoma (UC) is the second most common urological cancer, that can develop in both the lower (bladder and urethra) and the upper urinary tract (renal pelvis and ureter). Bladder cancer (BC) accounts for 90–95% of UCs whilst upper tract urothelial carcinomas (UTUC) account for only the remaining 5–10% (1).

1.1. Epidemiology of bladder cancer

BC presents a major challenge to global healthcare systems, ranking as the ninth most common cancer worldwide. According to the 2022 GLOBOCAN data, BC was responsible for nearly 615,000 new cases and 220,000 deaths in 2022 (2). The incidence and mortality rates of BC differ between countries due to differences in risk factors, screening and diagnostic methods, and availability of treatments. In developed countries, BC often presents higher incidence rates, partly due to lifestyle-related risk factors such as smoking and occupational exposures (3). Nine European countries are among the top ten for incidence rates and European countries also continue to dominate in terms of mortality rates (Table 1). Advanced healthcare systems in these regions facilitate early detection, which can improve survival rates. However, despite constantly developing treatment options, BC is still a significant cause of cancer-related deaths, especially among older adults. Hungary, with nearly 3,300 new cases and more than 1,000 deaths in 2022, ranks 11th for both incidence and mortality rates (Table 1).

Table 1. Top 10 countries (+ Hungary) by incidence (A) and mortality (B) rates of BC

A) Incidence				**B) Mortality**			
Rank	**Country**	**Number**	**Rate**	**Rank**	**Country**	**Number**	**Rate**
1	Italy	34,580	57.4	1	Greece	1,554	15.1
2	Greece	5,122	49.7	2	Poland	5,346	14.2
3	Spain	21,418	45.8	3	Italy	8,254	13.7
4	The Netherlands	7,835	45.5	4	Portugal	1,392	13.7
5	Denmark	2,501	42.9	5	Croatia	552	13.6
6	Canada	15,111	39.4	6	Spain	5,832	12.5
7	Switzerland	3,202	36.5	7	Slovenia	255	12.3
8	Portugal	3,517	34.7	8	France	7,934	12.1
9	Germany	29,035	34.6	9	Latvia	219	11.9
10	United Kingdom	23,643	34.5	10	The Netherlands	1,920	11.2
11	**Hungary**	**3,246**	**33.8**	**11**	**Hungary**	**1,063**	**11.1**

More than three times as many men as women were among the newly diagnosed BC cases in 2022 (2). Although men are more likely to develop BC, women tend to be diagnosed at a more advanced stage and have poorer prognosis (4).

1.2. Pathology

More than 90% of BCs are urothelial (transitional cell) carcinomas, with approximately 5% classified as squamous cell carcinomas, and less than 2% as adenocarcinomas. Non-epithelial tumor types occur much less frequently (5). Based on histological staging, BC can be classified into non-muscle-invasive (NMIBC) and muscle-invasive (MIBC) forms. About 70% of newly diagnosed cases are NMIBC, while in approximately 30% of patients, the tumor has already invaded the muscularis propria of the bladder wall. All MIBC cases are poorly differentiated, also referred to as high-grade UCs. Notably, NMIBC recurs frequently (in 50-70% of cases) after transurethral treatment, but it rarely progresses to MIBC (only in 10-20% of cases) and shows a good prognosis with over 90% 5-year cancer-specific survival (6, 7). MIBC patients, however, often face high rates of disease recurrence, progression, and mortality, even after undergoing comprehensive treatments such as radical surgery (cystectomy) and neoadjuvant or adjuvant therapies. Approximately 40% of these patients experience metastatic relapse, while 5% are initially diagnosed with metastatic disease (6, 8). The 5-year overall survival (OS) rate for metastatic UC (mUC) is around 9% (9).

1.3. Disease management of MIBC

For decades, the gold standard treatment for MIBC has been radical cystectomy (RCE) with extended pelvic lymph-node dissection. RCE is recommended for patients with muscle-invasive and clinically organ-confined tumors (≥cT2, N0-Nx, M0), very high-risk NMIBC, as well as extensive papillary disease that cannot be controlled with transurethral resection of the tumor and intravesical systematic therapy alone (10). However, RCE achieves a 5-year survival rate of only about 50% (11). To improve survival outcomes for patients with organ-confined (cN0M0) disease, cisplatin-based neoadjuvant chemotherapy (NAC) has been used since the 1980s. According to the latest guidelines, NAC is strongly recommended for MIBC patients who are eligible for cisplatin-based chemotherapy (12). Previous studies have shown that NAC can result in an 8% improvement in the 5-year survival rate, while having no impact on surgical morbidity (13, 14). Additionally, the neoadjuvant approach allows for early determination of *in vivo*

chemosensitivity. A disadvantage of NAC is the delay in local treatment for patients who do not show chemotherapy-sensitivity (15). Other compounds, such as immune checkpoint inhibitors (ICI), are increasingly being tested in the neoadjuvant setting, either as monotherapy or in combination with chemotherapy, showing promising results (16). However, this strategy has not yet received approval for routine clinical use.

For decades, platinum-based chemotherapy has been the standard first-line systematic treatment for MIBC. The latest guidelines still recommend strongly to offer adjuvant cisplatin-based combination chemotherapy to patients with locally advanced or metastatic disease if no NAC has been given before (12). A recent meta-analysis involving 1183 patients treated with adjuvant cisplatin-based chemotherapy has revealed an improvement in OS of 6% at 5 years. A part of these patients will progress to metastatic disease and the prognosis for mUC remains poor, with a median OS of only 12-14 months (17, 18). Moreover, up to 50% of patients are cisplatin ineligible due to poor performance status or comorbid conditions like renal or heart failure (19).

Lately, the treatment landscape for mUC has been significantly evolved. Recent randomized controlled trials and real-life studies have challenged the dominance of cisplatin-based chemotherapy, exploring the benefits of other systematic therapies such as ICIs, the FGFR-inhibitor erdafitinib, and the antibody-drug conjugates enfortumab vedotin and sacituzumab govitecan.

1.4. Immune checkpoint inhibitors

The reaction of the immune system to pathogenic organisms as well as self-antigens needs to be carefully regulated, ensuring the elimination of pathogens and cancerous cells, while also maintaining immune tolerance (20). Immune checkpoints play a pivotal role in maintaining a delicate balance between activation and suppression of this system. These molecular "brakes" are located on the surface of immune cells, including T lymphocytes, or on tumor cells and trigger different signals that regulate and prevent the over-activation of T cells (21). The 2018 Nobel Prize in Physiology or Medicine was awarded to Tasuku Honjo and James Allison for the discovery of the two most important immune checkpoints: PD-1 (Programmed Death-1) and CTLA-4 (Cytotoxic T-Lymphocyte Antigen-4). The inhibition of T cell activation by PD-1 and/or CTLA-4 is regarded as one of the key ways in which cancer cells evade immune detection. By blocking these molecules, the immune system can be reactivated to effectively fight cancer (22).

DOI:10.14753/SE.2025.3157

The activation of T lymphocytes, the effector cells of anti-tumor immunity, requires multiple signals. The first signal consists of the connection of MHC-presenting antigen to T cell receptor (TCR). The other stimulus is provided by co-stimulatory and co-inhibitory signals (23). The interaction between PD-1 on T cells and PD-L1 on tumor cells or antigen-presenting cells (APCs) can strongly inhibit T cell activation, leading to T cell apoptosis, reduced cytokine production, impaired T cell lysis, and the induction of antigen tolerance (24). This interaction allows tumors to evade immune surveillance. Anti-PD-(L)1 antibodies block the binding of PD-1 to PD-L1, restoring the immune cells' ability to recognize and destroy cancerous cells (25) (Figure 1).

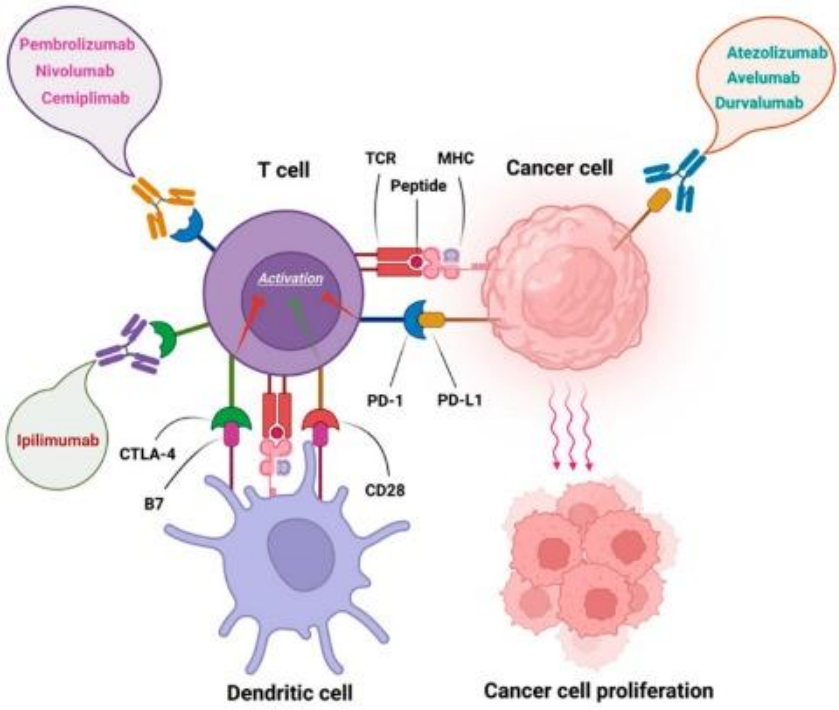

Figure 1. FDA-approved immune checkpoint inhibitors and their mechanism of action (25)

Pembrolizumab was the first anti-PD-1 inhibitor approved by the US Food and Drug Administration (FDA) in 2014 for the treatment of unresectable or metastatic melanoma (26). Later, the potential field of application was expanded to numerous other cancer types such as advanced non-small cell lung cancer, recurrent or metastatic head and neck squamous cell carcinoma, gastric cancer, ovarian cancer, and others (27, 28). In May 2017, right after the FDA-approval of the anti-PD-L1 inhibitor atezolizumab, the FDA granted accelerated approval to pembrolizumab for the treatment of patients with locally

advanced or metastatic UC, who are not eligible for cisplatin-containing chemotherapy (29, 30). The potential field of application was soon further expanded to the post-platinum setting. Prospective clinical trials such as the IMvigor210 and KEYNOTE-045 served as the basis for approval (31, 32). Other ICI drugs such as avelumab or nivolumab have also been approved for certain mUC settings (33, 34). Despite the promising results of the first clinical trials, the application of ICIs has faced some challenges (35). Early results from trials KEYNOTE-361 and IMvigor130 indicated that patients receiving pembrolizumab or atezolizumab as first-line monotherapy had inferior survival to those on traditional cisplatin- or carboplatin-based treatments (36, 37). Consequently, the use of these ICI monotherapy (pembrolizumab) in the first-line setting has been restricted to cisplatin ineligible patients with high levels of PD-L1 protein expression (38). A summary of the most important clinical trials of different ICI drugs in UC is presented in Table 2.

The clinical trials involved carefully selected and well-defined patient groups, conducted under standardized and strictly controlled conditions to reduce bias and potential confounding factors (39). However, since the trial population may differ in many ways (age, comorbidities, generalized organ dysfunction) from those seen in everyday clinical practice, the results may not apply to all populations (40). Therefore, there is a need for real-world data primarily from electronic medical records to assess the efficacy of ICI treatment in the general population.

Table 2. Summary of key clinical trials of ICIs in UC

Study	Year	Drug	Phase	Population	Comparator	Primary endpoint	Key findings	FDA approval	Reference
IMvigor210	2016	Atezolizumab	Phase II	Advanced UC, post-platinum (Cohort 2) and cisplatin-ineligible (Cohort 1)	Single-arm study	ORR	Showed ORR of 16% in post-platinum patients (Cohort 2) and 23% in cisplatin-ineligible patients (Cohort 1).	Approved for post-platinum and cisplatin-ineligible patients (2016, accelerated approval).	Rosenberg *et al.* (2016)
KEYNOTE-052	2017	Pembrolizumab	Phase II	Advanced UC, cisplatin-ineligible	Single-arm study	ORR	ORR of 29%, with higher responses (33%) in PD-L1+ patients.	Approved for cisplatin-ineligible patients (2017, accelerated approval).	Balar *et al.* (2017)
IMvigor211	2017	Atezolizumab	Phase III	Advanced UC, post-platinum chemotherapy	Chemotherapy	OS	No significant OS benefit in intent-to-treat population; higher OS in high PD-L1 expression subgroup.	No additional approval.	Powles *et al.* (2017)
KEYNOTE-045	2017	Pembrolizumab	Phase III	Advanced UC, post-platinum chemotherapy	Chemotherapy	OS	Pembrolizumab improved OS compared to chemotherapy (10.3 vs. 7.4 months).	Approved for post-platinum chemotherapy setting (2017).	Bellmunt *et al.* (2017)
IMvigor130	2019	Atezolizumab ± Chemotherapy	Phase III	Untreated advanced UC	Chemotherapy	OS and PFS	Atezolizumab + chemotherapy improved PFS but did not meet OS significance threshold.	No additional approval.	Galsky *et al.* (2020)
KEYNOTE-361	2020	Pembrolizumab ± Chemotherapy	Phase III	Untreated advanced UC	Chemotherapy	OS and PFS	Did not show superiority of pembrolizumab + chemotherapy over chemotherapy alone in OS and PFS.	No additional approval.	Powles *et al.* (2021)
JAVELIN Bladder 100	2020	Avelumab	Phase III	Advanced UC, post-platinum response	Best supportive care (BSC)	OS	Avelumab maintenance significantly improved OS compared to BSC (median OS 21.4 vs. 14.3 months).	Approved for maintenance therapy in post-platinum patients (2020).	Powles *et al.* (2022)
CheckMate 274	2021	Nivolumab	Phase III	Muscle-invasive UC post-cystectomy	Placebo	Disease-free survival (DFS)	Significant improvement in DFS in both PD-L1+ and all-comers populations (median DFS 20.8 vs. 10.9 months).	Approved for adjuvant therapy post-cystectomy (2021).	Bajorin *et al.* (2021)

Although PD-(L)1 inhibitors have shown impressive efficacy in a subset of UC patients, challenges such as drug resistance and side effects persist. About only 20–30% of mUC patients benefit from the ICI therapy, and fewer patients could experience durable responses lasting more than 2 years. In addition, a remarkable subset of patients can face serious immune-related side effects (41). These facts highlight the growing need for reliable biomarkers to guide treatment selection and better predict which patients are most likely to benefit from ICI therapy (42).

1.5. Immune checkpoint inhibitor therapy predictive markers in UC

1.5.1. PD-L1 tissue expression

One of the most extensively studied predictive biomarkers in mUC is PD-L1 tissue expression determined by immunohistochemistry (IHC). However, clinical trial data varied markedly, underscoring the challenge of relying on PD-L1 IHC scores as standalone predictive biomarker (31, 32, 43, 44). The use of different antibodies and various scoring systems may at least partly explain the lack of reproducibility of PD-L1 IHC (45, 46). In addition, PD-L1 expression can be transient and heterogeneous

influenced by various molecular mechanisms within both the tumor and its microenvironment (47-49). Conflicting results regarding the correlation between PD-L1 expression and patient survival may arise from both technical challenges and the dynamic regulation of PD-L1 expression. The major limitation of PD-L1 staining relates to the significant proportion of PD-L1-negative patients who respond to ICIs. Thus, the adequate predictive value of PD-L1 could not be confirmed in large trials (36, 50).

Enzymes such as matrix metalloproteinases can cleave the extracellular domain of PD-L1, resulting in soluble forms detectable in blood samples from both healthy individuals and cancer patients (51). Recent studies have suggested a potential prognostic role for sPD-L1 in various cancer types (52, 53); however, limited data are available regarding its role as a biomarker in UC.

1.5.2. Tumor mutational burden (TMB)

High TMB through increasing neoantigen load potentially enhances the tumor's immunogenicity and response to ICI therapy (54). Somatic mutation rates proved to be usually higher in cancers associated with long-term carcinogenic exposure, including UC (55). High TMB has been correlated with improved response rates and prolonged survival in mUC (31, 56, 57). However, the promising results from small single-arm studies need further validation.

1.5.3. Molecular subtypes of BC

Based on their gene expression patterns urothelial BCs can be classified into different molecular subtypes. The gene signatures that specify the subtypes are diverse, covering signatures such as epithelial differentiation, stromal involvement, cell cycle activity, and immune cell infiltration (58). Multiple classification systems have been developed to identify and define molecular subgroups of BC (Figure 2) (59).

Gene expression-based molecular subtypes according to various classification systems have also been suggested to show differences in treatment outcomes to ICI therapy. However, studies reported rather controversial results. According to consensus classification system favourable responses to ICI (atezolizumab) could be observed among patients with luminal non-specified (LumNS), luminal unstable (LumU), and neuroendocrine like (NE-like) tumors (60). The TCGA classification system distinguished five different subtypes, of which the luminal-infiltrated group was characterized by high immune/stromal infiltration and high expression of PD-L1. Thus,

it has been speculated as ICI responsive subtype (61, 62). However, validation studies using the same classification system have shown that the luminal and the neuronal subtypes derive the most benefit from ICI therapy (63, 64). The relationship between molecular subtypes and response to ICI therapy is still an area of active research, and further studies are needed to validate previous findings. Despite many promising associations with clinical outcomes and treatment response, its clinical impact has yet to be defined.

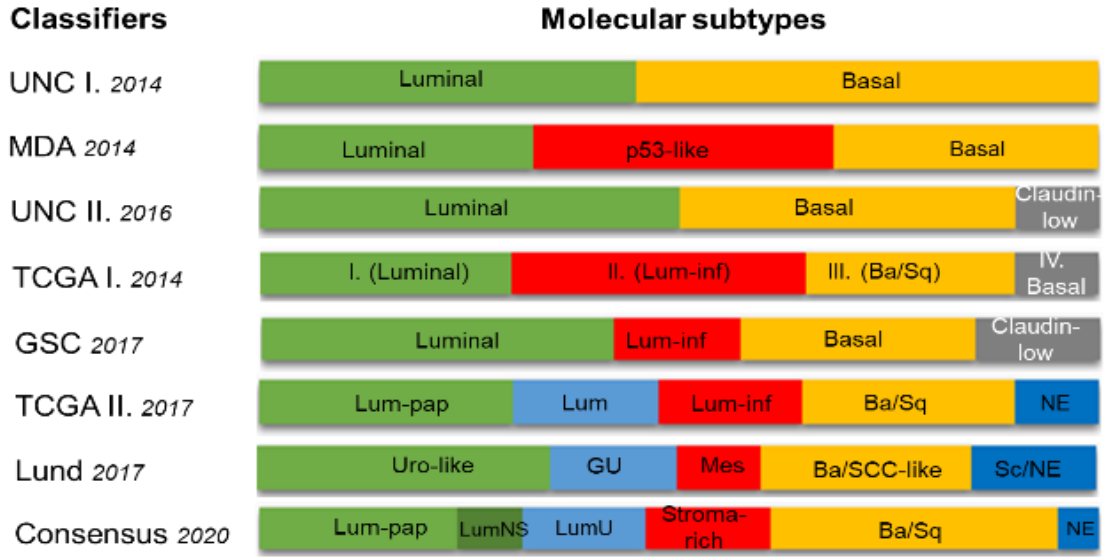

Figure 2. Gene expression-based molecular subtype classification of muscle-invasive bladder cancers, as recommended by various research groups (59).
Ba/SCC-like: basal/squamous cell carcinoma, Ba/Sq: basal/squamous, Lum: luminal, Lum-inf: luminal-infiltrated, LumNS: non-specified luminal, Lum-pap: luminal-papillary, LumU: luminal unstable, Mes: mesenchymal-like, GU: genomically unstable, Ne: neuronal, Sc/Ne: small-cell/neuroendocrine-like, Uro-like: urothelial-like.

Other investigated markers such as CD8 expression and other immune gene cell signatures (65) showed limited results. The predictive value of standalone biomarkers seems to be restricted and can be influenced by various factors, including the dynamics of the tumor microenvironment, treatment history, and interpatient variability. Additionally, the lack of standardization in biomarker assessment methods and scoring systems can further complicate the interpretation of results and limit their clinical utility. To address these challenges, the use of integrative approaches that combine various clinicopathological, molecular, and immune-related factors is essential to improve predictive accuracy. As the therapeutic landscape for mUC continues to evolve, the

DOI:10.14753/SE.2025.3157

development of robust and clinically relevant biomarkers remains crucial for refining patient selection and optimizing treatment outcomes.

DOI:10.14753/SE.2025.3157

2. Objectives

The aim of the study is to gain a better understanding of the factors affecting the effectiveness of ICI therapy under real-world conditions and to identify new potential predictive molecular markers or set of markers. The work presented here has two main parts: clinical data analysis and molecular analyses (Figure 3).

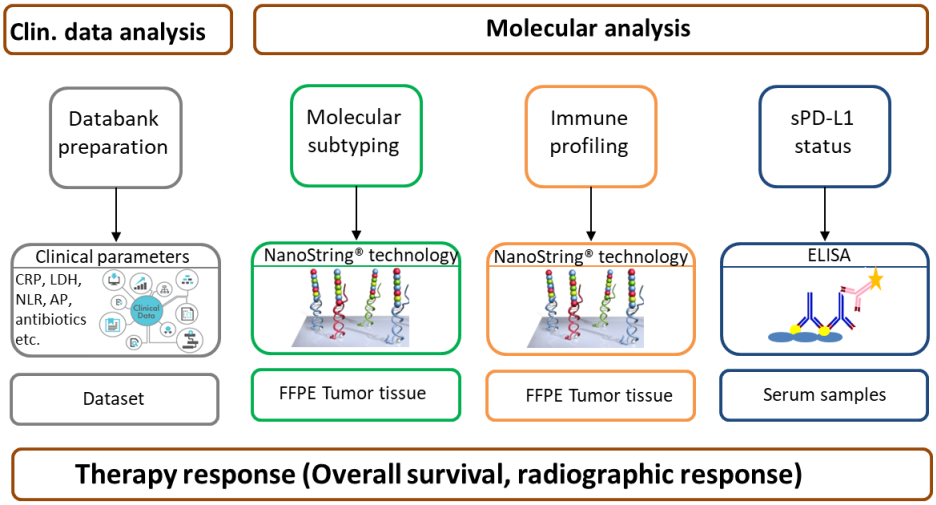

Figure 3. Overview of the research plan (Own figure)

2.1. Aims of the retrospective clinical data analysis

This multicentric, retrospective study aimed:

1. To assess the characteristics of UC patients receiving ICI treatment in routine clinical settings.
2. To compare the effectiveness of two widely used ICI drugs (pembrolizumab and atezolizumab) against results from respective clinical trials.
3. To evaluate the prognostic significance of standard clinicopathological and laboratory parameters.

2.2. Aims of the molecular analyses

1. To identify potential ICI-predictive genes in our institutional UC patient cohort through gene expression analysis of the tumor and its microenvironment.
2. To develop a prognostic model by combining clinicopathological and molecular factors.
3. To examine how different molecular subtypes of UC relate to therapy response and survival outcomes in patients undergoing ICI treatment
4. To evaluate the prognostic value of soluble PD-L1 (sPD-L1) as a serum biomarker

3. Methods

3.1. Clinical data analysis

3.1.1. Patients and data collection

Eligible patients included adults (≥18 years) with a confirmed diagnosis of advanced or metastatic urothelial tract malignancy who received at least one cycle of ICI (pembrolizumab or atezolizumab) as first-, second-, or later-line treatment between January 2017 and December 2021. Exclusion criteria included histological variants other than UC, combination therapy, monotherapy with nivolumab, avelumab, or durvalumab, and ICI in the neoadjuvant setting (Figure 4). Patient data were obtained from medical records and respective files across 6 uro-oncology centers (Semmelweis University; National Institute of Oncology; Borsod-Abaúj-Zemplén County University Hospital, University Hospital Düsseldorf; University Hospital Essen; University of Szeged), collecting clinicopathological, laboratory (if available), and clinical outcome data.

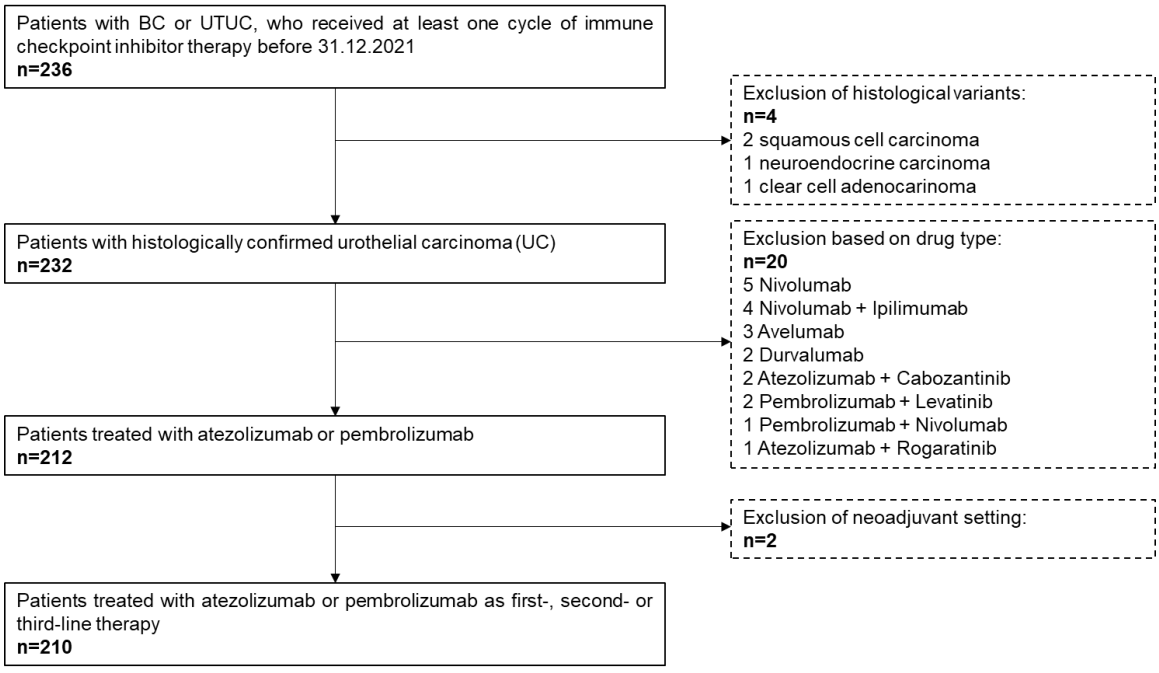

Figure 4. Flow chart of the patient selection.(115)
Figure 4 has been published in the article: Váradi M. et al. Efficacy of immune checkpoint inhibitor therapy for advanced urothelial carcinoma in real-life clinical practice: results of a multicentric, retrospective study. Sci Rep. 2023 Oct 13;13(1):17378.

Cut-off values for laboratory parameters were primarily derived from previous studies: hemoglobin (10 g/dL), C-reactive protein (CRP, 30 mg/L), and neutrophil-lymphocyte ratio (NLR, 5) were set according to the original and enhanced Bellmunt risk score (66,

67). In addition, the lower limit of the normal range was employed as the cut-off value for albumin (35 g/l), and the upper limit of the normal range as the cut-off for LDH (250 U/l). In the case of estimated glomerular filtration rate (eGFR), we applied two different cut-off values 50 ml/min and 40 ml/min respectively. The end date for data analysis was August 2022.

The study conformed to the Declaration of Helsinki, and the regional ethics committee approved the protocol (approval no.: SE RKEB 125/2019).

3.1.2. Outcomes

Overall survival (OS) was used as the primary endpoint of this study because it is a robust and objective endpoint; moreover, information on response and progression was not always available. Secondary outcomes included progression-free survival (PFS), objective response rate (ORR), disease control rate (DCR), and duration of response (DOR).

OS was defined as the period from the initiation of ICI therapy to the date of death from any cause, while PFS was defined as the time from the first ICI treatment to the date of disease progression (radiographic or clinical) or death from any cause. Patients who did not die were censored at the time of the last follow-up.

Responses were assessed by computed tomography (CT), with evaluation performed by local radiologists at each center according to Response Evaluation Criteria in Solid Tumors (RECIST) guideline version 1.1 (local guidelines). Treatment response was determined by the data collector based on radiographic studies and clinical notes. ORR was defined as the percentage of patients achieving a partial or complete response (PR or CR) to treatment within the follow-up period, while DCR referred to the proportion of patients with CR, PR, or stable disease (SD). Time to response was defined as the duration from the first cycle to the first documented response. DOR was defined as the time from the first documented radiological response to disease progression or death from any cause, whichever occurred first.

3.1.3. Statistical analysis

Descriptive statistics included the median and range for continuous variables and counts with percentages for categorical variables. All time-to-event data (OS, PFS, DOR) were visualized using Kaplan-Meier estimates, with medians reported alongside corresponding

95% confidence intervals (CIs). The median and range of time to response were reported for patients with CR and PR. Cox proportional hazards models were used to assess differences in hazard ratios (HRs) between groups according to risk factors, and a stratified two-sided log-rank test was employed to assess differences in OS. A Chi-Squared Test of Independence was conducted to determine associations between response (CR/PR) or disease control (CR/PR/SD) and various clinicopathological variables. A p-value of <0.05 was considered statistically significant. All statistical analyses were performed with IBM SPSS Statistics, version 27.0 (IBM Corp., Armonk, NY, USA).

3.2. Molecular analyses – gene expression analysis

3.2.1. Samples and data collection

The study included advanced or metastatic UC patients with available formalin-fixed, paraffin-embedded (FFPE) tumor samples, who received at least one cycle of ICI therapy (pembrolizumab or atezolizumab) as first- or second-line treatment between January 2017 and February 2023. Patients with low-quality tumor tissue samples or lacking follow-up data were excluded (Figure 5).

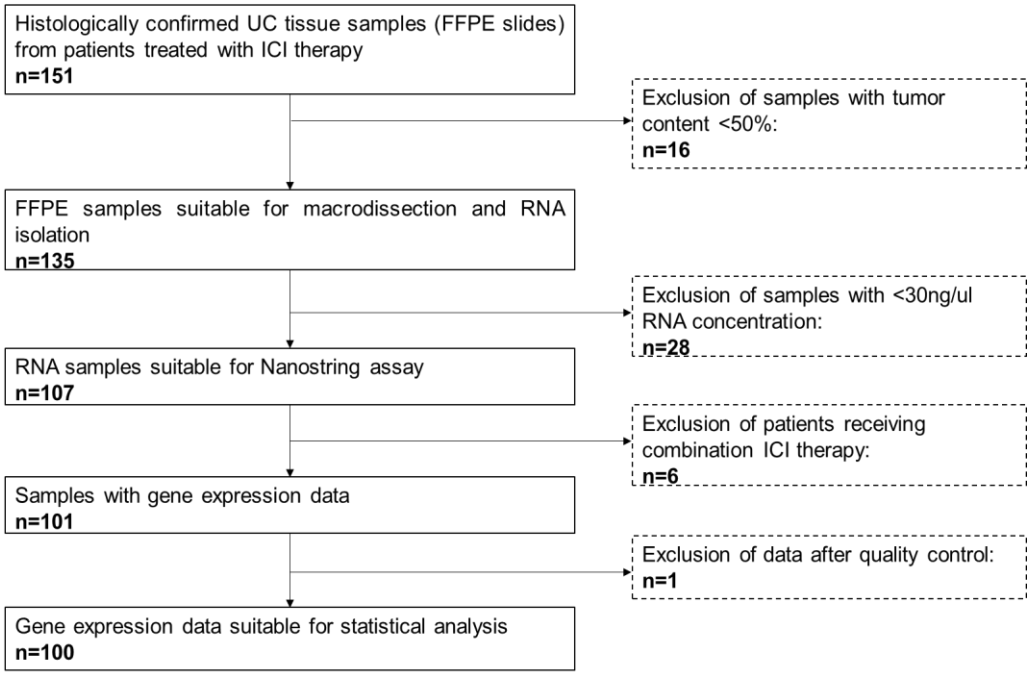

Figure 5. Flow chart of the sample selection (Own figure)

Data were obtained from medical records at six uro-oncology centers (Semmelweis University; National Institute of Oncology; University Hospital Düsseldorf; University Hospital Essen; University of Szeged; University Hospital Frankfurt) as previously

described. The follow-up cut-off was at 11/2023. The study conformed to the Declaration of Helsinki, and the respective ethics committees (Semmelweis University Regional and Institutional Committee of Science and Research Ethics, and the Ethics Commission of the Medical Faculty of the University of Duisburg-Essen) approved the study protocol (SE RKEB 125/2019, 15–6400-BO, 2021–1548).

3.2.2. RNA extraction and gene expression profiling

Samples from radical surgeries (cystectomy or nephroureterectomy) or transurethral bladder resections were prepared for gene expression analysis. RNA was extracted from 10 μm-thick FFPE tissue sections (2–10 slides per case). To reduce contamination with non-malignant tissue, macrodissection was performed, focusing only on marked tumor areas with >50% tumor cell content. A board-certified genitourinary pathologist identified these tumor areas on hematoxylin and eosin (H&E)-stained slides. Selected areas were carefully scraped, and RNA was isolated using the MagMAX™ FFPE DNA/RNA Ultra Kit (Thermo Fisher Scientific, Waltham, MA, USA) per the manufacturer's protocol. Extracted RNA concentrations were measured with the Qubit™ RNA High-Sensitivity Assay Kit and the Qubit fluorometer (Thermo Fisher Scientific, Waltham, MA, USA).

Samples with sufficient RNA concentrations (>30 ng/μL) were hybridized to the NanoString nCounter® PanCancer IO 360™ Gene Expression Panel (NanoString, Seattle, WA, USA) for 24 hours in a thermocycler. Samples were processed on the nCounter Prep Station (NanoString, Seattle, WA, USA), and gene expression profiles were digitized using the nCounter Digital Analyzer.

3.2.3. Molecular subtype classification

For molecular subtype classification according to the MDA, Lund, TCGA and consensus classification systems, we used a gene panel based approach with 48 genes covering six tumor cell-specific (luminal, basal, squamous, neuronal, epithelial-to-mesenchymal transition (EMT), and in situ carcinoma [CIS]) as well as three stroma-related gene signatures (p53, extracellular matrix (ECM)/smooth muscle (SM), and immune cell-specific) (Table 3) (68, 69). NanoString nCounter® analysis with a custom gene panel of 48 subtype-specific genes and 19 additional single genes was conducted, as previously described.

Table 3. Applied gene set assigned to signatures and to classification systems (68,69).

Classification system				Signature	Selected genes									
TCGA II	MDA	LUND	Consensus											
X	X	X	X	Luminal	*CYP2J2*	*ERBB2*	*FGFR3*	*FOXA1*	*GATA3*	*KRT20*	*PPARG*	*UPK1A*	*UPK2*	-
X	X	X	X	Basal/Squamous	*CD44*	*CDH3*	*KRT14*	*KRT5*	*KRT6A*	*DSC2*	*DSG3*	*PI3*	-	-
X	-	X	X	Neuronal-diff.	*APLP1*	*CHGB*	*ENO2*	*GNG4*	*MSI1*	*PEG10*	*PLEKHG4B*	*RND2*	*SV2A*	*TUBB2B*
X	-	-	X	CIS	*CRTAC1*	*CTSE*	*MSN*	*NR3C1*	-	-	-	-	-	-
X	X	X	X	EMT	*CDH2*	*TWIST1*	*VIM*	*ZEB1*	-	-	-	-	-	-
X	X	X	X	ECM/SM	*COMP*	*SFRP4*	*SGCD*	-	-	-	-	-	-	-
X	-	-	-	Immune	*CD274*	*CXCL11*	*IDO1*	*SAA1*	-	-	-	-	-	-
-	X	-	-	p53	*ACTC1*	*ACTG2*	*CNN1*	*MYH11*	*PGM5*	-	-	-	-	-
-	-	X	X	Additional	*CDKN2A*	-	-	-	-	-	-	-	-	-
Additional single genes on the panel					*ACVR1*	*APOBEC3A*	*APOBEC3B*	*APOBEC3G*	*ARID1A*	*B2M*	*CALR*	*CIITA*	*EGFR*	*ERAP1*
					FLT4	*KI67*	*MMP7*	*NKG7*	*PDGFA*	*RB1*	*SLAMF6*	*TAGAP*	*TGFBR2*	-

3.2.4. Gene expression data analysis

The NanoString data analysis was conducted within the R for Windows environment (v4.4.0, R Foundation for Statistical Computing, Vienna, Austria, 2024). Log2 fold change (log2FC) calculations were manually performed, while normalized NanoString data (differential expression analysis) was compared using Wilcoxon rank-sum tests. For parameters with more than two levels, pairwise Wilcoxon rank-sum tests with Holm-corrected p-values (70) were used. Gene set enrichment analysis was also performed on data from the nCounter® PanCancer Immune Profiling Panel. Survival analysis utilized Cox regression models. Optimal cut-off values for each gene were determined by first calculating the upper (Q3) and lower (Q1) quartiles of each gene's expression values, then identifying the best cut-off between these quartiles using Cox regression analysis, and adjusting p-values with the Benjamini-Hochberg False-Discovery Rate (FDR). All p-values were FDR-corrected using the Benjamini- Hochberg method (71). Visualizations, including boxplots and heatmaps, were created with the ggplot2 (v3.5.1) and ComplexHeatmap (v2.20.0) R-packages, respectively. The Random Survival Forest (RSF) model was used to combine the significant factors identified from the univariate analysis to predict survival outcomes. The model was trained using the selected variables and the survival data, which included time-to-event information and censoring indicators. Model performance was assessed using Receiver Operating Characteristic (ROC) analysis, with the Area Under the Curve (AUC) calculated to evaluate the discriminatory ability of the RSF model. Additionally, C-statistics were calculated to assess the overall performance of the model. All analyses were performed in R with the randomForestSRC and pROC packages. To validate the prognostic value of selected genes, the online tool "Kaplan-Meier Plotter" (www.kmplot.com; accessed on 09/06/2024) was used to analyze

publicly available gene expression and survival data across cancer datasets, including ICI-treated UC cases. Additionally, the "ROC Plotter" tool (www.rocplot.com/immune; accessed on 09/06/2024) was employed to assess the diagnostic and predictive performance of differentially expressed genes, utilizing a database of 1,434 tumor tissue samples from 19 datasets that include esophageal, gastric, head and neck, lung, melanoma, and UC cancers (72). Both pan-cancer and UC-specific (IMvigor210) validations were performed.

3.3. Molecular analyses – determination of sPD-L1 levels

3.3.1. Patients and samples

Pre-treatment serum samples were collected from 12 UC patients who underwent ICI therapy with either atezolizumab (n = 11) or pembrolizumab (n = 1). Blood samples were collected in 9 mL Vacuette® tubes with the assistance of clinic nurses. After resting at room temperature for 30–90 minutes, tubes for serum preparation were centrifuged at 1500 rcf for 10 minutes. Then, 3 x 1000 µL of serum was pipetted into labelled Eppendorf tubes and stored at -80°C until use. Ten patients received ICI therapy as a second-line treatment, while 2 were treated due to platinum ineligibility. The samples were obtained between April 2019 and March 2020 at the Department of Urology, Semmelweis University. On-treatment serum samples, collected before the second immunotherapy cycle, were available for 92% (11/12) of the patients. The study was conducted in accordance with the Helsinki Declaration and approved by the institutional ethics committee (TUKEB 55/2014 and 224/2013). Written informed consent of all patients was available.

3.3.2. Serum PD-L1 Enzyme-Linked Immunosorbent Assay (ELISA)

Soluble PD-L1 levels in serum samples were measured using the PD-L1/B7-H1 Quantikine ELISA kit (DB7H10, R&D Systems, Wiesbaden, Germany) following the manufacturer's protocol. The ELISA plates were read using the Thermo Scientific™ Multiscan FC Microplate Photometer with SkanIt 5.0 Software. For dichotomization, the cut-off values were defined as the median (90 pg/mL). To rule out potential interference or cross-reactivity between the therapeutic anti-PD-L1 antibody (atezolizumab, Tecentriq®, Roche, Basel, Switzerland) and the ELISA kit, additional ELISA analyses

DOI:10.14753/SE.2025.3157

were performed using atezolizumab and pembrolizumab. The low number of cases did not allow a valid statistical analysis.

DOI:10.14753/SE.2025.3157

4. Results

4.1. Clinical data analysis

4.1.1. Patient characteristics

Data from 210 eligible patients were analyzed. A full description of patient characteristics for the whole cohort, as well as for the first- and second-line cohorts, is provided in Table 4.

Seventy-six patients received atezolizumab, and 134 patients received pembrolizumab. The median age at the start of ICI therapy was 67.3 years (range: 28.9–87.2 years). The most common primary tumor localization was in the bladder, affecting 81.9% (n=172) of patients. Twelve cases (5.7%) presented with tumors in both locations (upper urinary tract and bladder). Ninety-one patients (43.3%) underwent radical surgery (cystectomy or nephroureterectomy), and 22 patients (10.5%) received radiochemotherapy as local treatment. At the time of ICI initiation, 31.9% of patients had lymph node-only metastases, and 45.2% had visceral metastases. The majority of patients (83.3%) were categorized into ECOG PS groups 0-1.

We had sufficient data for 184 patients to classify them according to the Bellmunt criteria. The Bellmunt risk score classifies patients into risk groups based on three factors: ECOG PS >0, hemoglobin (Hgb) level <10 g/dL, and the presence of liver metastases (67). The distribution of risk groups was as follows: 35.2% had no risk factors (Bellmunt 0), 38.6% had one risk factor (Bellmunt 1), 11.4% had two risk factors (Bellmunt 2), and 2.4% (5 patients) had three risk factors (Bellmunt 3). In the first-line cohort, more than half of the patients had at least one risk factor.

Table 4. Patient characteristics. *Table 4 has been published in the article: Váradi M. et al. Efficacy of immune checkpoint inhibitor therapy for advanced urothelial carcinoma in real-life clinical practice: results of a multicentric, retrospective study. Sci Rep. 2023 Oct 13;13(1):17378.* (115)

Variables		Whole cohort n (%)	First-line n (%)	Second-line n (%)
Total number of patients		210	84	126
Age at diagnosis, years median (range)		67.3 (28.9-87.2)	70.0 (45.2-87.2)	65.3 (28.9-86.3)
Age at ICI initiation, years median (range)		69.8 (29.4-88.8)	71.9 (45.3-88.4)	68.2 (29.4-88.8)
Sex	Male	146 (69.5)	51 (60.7)	95 (75.4)
	Female	64 (30.5)	33 (39.3)	31 (24.6)
Location of primary tumor	UTUC	26 (12.4)	6 (7.1)	20 (15.9)
	BC	172 (81.9)	74 (88.1)	98 (77.8)
	Both	12 (5.7)	4 (4.8)	8 (6.3)
Setting	1L	84 (40.0)	84 (100.0)	-
	2L	126 (60.0)	-	126 (100.0)
Drug	Atezolizumab	76 (36.2)	18 (21.4)	58 (46.0)
	Pembrolizumab	134 (63.8)	66 (78.6)	68 (54.0)
Prior treatments	NAC	20 (9.5)	7 (8.3)	13 (10.3)
	RCE	63 (30.0)	22 (26.2)	41 (32.5)
	RNU	28 (13.3)	8 (9.5)	20 (15.9)
	CTX (IC/AC/PC)	126 (60.0)	-	126 (100.0)
	RCT	22 (10.5)	18 (21.4)	4 (3.2)
	RT	77 (36.7)	38 (45.2)	39 (31.0)
ECOG-PS at ICI initiation	0	117 (55.7)	39 (46.4)	78 (61.9)
	1	58 (27.6)	28 (33.3)	30 (23.8)
	2	22 (10.5)	15 (17.9)	7 (5.6)
	3	2 (1.0)	-	2 (1.6)
	Unknown	11 (5.2)	2 (2.4)	9 (7.1)
Metastatic sites	LN	144 (68.6)	55 (65.5)	89 (70.6)
	Only LN	67 (31.9)	29 (34.5)	38 (30.2)
	Liver	33 (15.7)	9 (10.7)	24 (19.0)
	Visceral	95 (45.2)	32 (38.1)	63 (50.0)
	Bone	49 (23.3)	9 (10.7)	40 (31.7)
	No metastases	22 (10.5)	16 (19.0)	6 (4.8)
Bellmunt risk factors	0	74 (35.2)	19 (22.6)	55 (43.7)
	1	81 (38.6)	43 (51.2)	38 (30.2)
	2	24 (11.4)	9 (10.7)	15 (11.9)
	3	5 (2.4)	-	5 (4.0)
	Unknown	26 (12.4)	13 (15.5)	13 (10.3)

ICI: immune checkpoint inhibitor, UTUC: upper tract urothelial carcinoma, BC: bladder cancer, 1L: first-line, 2L: second-line, NAC: neoadjuvant chemotherapy, RCE: radical cystectomy, RNU: radical nephroureterectomy, CTX: chemotherapy, IC: induction chemotherapy, AC: adjuvant chemotherapy, PC: palliative chemotherapy, RCT: radiochemotherapy, RT: radiotherapy, ECOG-PS: Eastern Cooperative Oncology Group performance status, LN: lymph node

4.1.2. Real-world efficacy (tumor responses, PFS, OS) of ICIs

Patients received a median of 6 treatment cycles (range: 1–80) and remained on therapy for a median of 4.3 months. At the time of the data cut-off, 31 patients (14.8%) were still receiving ICI therapy. The primary reason for discontinuing treatment was disease progression. The median follow-up period after ICI initiation was 10.2 months. No

radiographic response data was available for 29 patients. Among the 181 patients evaluable for radiographic response, 13 achieved a complete response, and 53 had a partial response. The overall response rate (ORR) for the entire cohort was 36.5%, with ORRs of 32.9% in the first-line setting and 38.9% in the second-line setting. The median duration of response (DOR) was 11.8 months. Disease control was achieved in 112 patients, resulting in a disease control rate (DCR) of 61.9% for the entire cohort.

The median PFS was 5.9 months (95% CI: 3.9–7.8 months). For first-line ICI treatment, the median PFS was 7.2 months (95% CI: 4.2–10.3 months), while for second-line treatment, it was nearly 3 months shorter, at 4.4 months (95% CI: 2.3–6.5 months). A total of 140 patients (66.7%) died during the study period. The median OS was 13.6 months (95% CI: 9.4–17.7 months). Tumor responses, and survival data for the whole cohort, as well as the first- and second-line cohorts, are shown in Table 5.

Table 5. Follow-up characteristic and tumor response. *Table 5 has been published in the article: Váradi M. et al. Efficacy of immune checkpoint inhibitor therapy for advanced urothelial carcinoma in real-life clinical practice: results of a multicentric, retrospective study. Sci Rep. 2023 Oct 13;13(1):17378.* (115)

	Whole cohort	**First-line**	**Second-line**
Variables	**n (%)**	**n (%)**	**n (%)**
Time of follow-up, months, median (range)	10.2 (0-68.7)	10.2 (0.5-68.7)	10.2 (0-64.8)
Number of cycles of ICI, median	6 (1-80)	7 (1-47)	5 (1-80)
ICI treatment (months), median (range)	4.3 (0-54.6)	4.95 (0-31.8)	3.6 (0-54.6)
ICI treatment ongoing at last follow-up	31 (14.8)	13 (15.5)	18 (14.3)
Best overall response			
Complete response (CR)	13 (7.2)	8 (11.0)	5 (4.6)
Partial response (PR)	53 (29.3)	16 (21.9)	37 (34.3)
Stable disease (SD)	46 (25.4)	24 (32.9)	22 (20.4)
Progressive disease (PD)	69 (38.1)	25 (34.2)	44 (40.7)
No radiologic evaluation performed	29	11	18
ORR	66 (36.5)	24 (32.9)	42 (38.9)
DCR	112 (61.9)	48 (65.8)	64 (59.3)
DOR, months, median (range)	11.8 (0.1-67.7)	11.4 (0.4-67.7)	11.9 (0.1-62.9)
PFS, months, median (95% CI)	5.9 (3.9-7.8)	7.2 (4.2-10.3)	4.4 (2.3-6.5)
Death at last follow-up	140 (66.7)	50 (59.5)	90 (71.4)
OS, months, median (95% CI)	13.6 (9.4-17.7)	13.7 (10.0-17.5)	13.6 (7.2-19.9)

ICI: immune checkpoint inhibitor, ORR: overall response rate, DCR: disease control rate, DOR: duration of response, PFS: progression-free survival, OS: overall survival, CI: confidence interval

4.1.3. Determinants of OS and PFS

In univariate Cox regression analysis, radical surgery, only lymph node metastases, high hemoglobin, albumin, and eGFR levels prior to therapy initiation were significantly

associated with improved OS. In contrast, the presence of liver metastases, visceral metastases or bone metastases, impaired ECOG PS, the presence of any Bellmunt risk factor, and elevated NLR values (≥5) were identified as prognostic factors for shorter OS, as shown in Table 6.

In Cox regression analysis examining PFS, age over 68 years at ICI initiation, lymph node metastases, hemoglobin, and albumin levels above the cut-off were associated with improved PFS. On the other hand, the presence of liver metastases, visceral metastases, bone metastases, ECOG PS > 0, NLR ≥5 and Bellmunt risk group 1+ (Figure 6) were associated with worse PFS, as shown in Table 6. Univariate Cox regression analyses were also performed separately for the first- and second-line treatment groups, with the results for the second-line subgroup being similar to those for the whole cohort (Table 7).

The multivariable analysis included all variables that showed a significant association with survival and for which data were available for at least 85% of cases. In multivariate analysis, ECOG PS, the presence of visceral or bone metastases, and hemoglobin levels ≥10 g/dL were identified as independent prognostic factors for OS. The presence of one

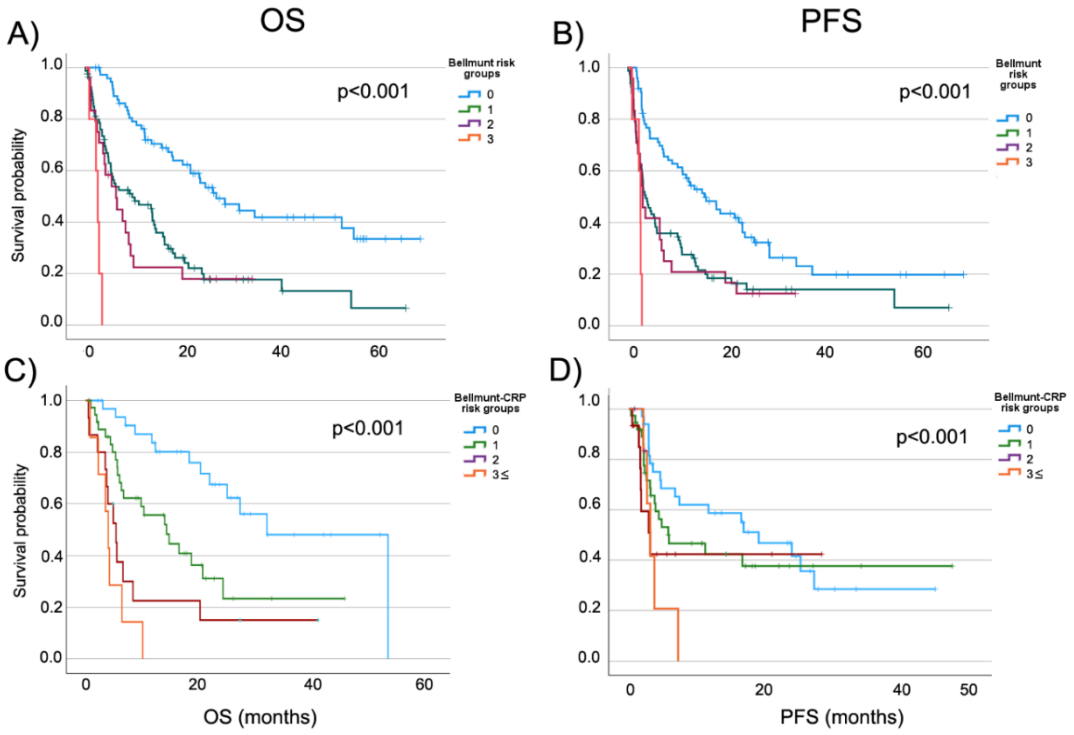

Figure 6. Overall survival (OS) (left) and progression-free survival (PFS) (right) for patients grouped according to Bellmunt risk factors (**A**,**B**) and Bellmunt-CRP risk factors (**C**,**D**). (115)
Figure 6 has been published in the article: Váradi M. et al. Efficacy of immune checkpoint inhibitor therapy for advanced urothelial carcinoma in real-life clinical practice: results of a multicentric, retrospective study. Sci Rep. 2023 Oct 13;13(1):17378.

or more Bellmunt risk factors was found to be an independent prognostic factor for shorter OS and PFS as well (Table 8).

Table 6. Univariate Cox regression analysis for the whole cohort. *Table 6 has been published in the article: Váradi M. et al. Efficacy of immune checkpoint inhibitor therapy for advanced urothelial carcinoma in real-life clinical practice: results of a multicentric, retrospective study. Sci Rep. 2023 Oct 13;13(1):17378.* (115)

		Overall survival				Progression-free survival			
Variables		**n**	**HR**	**95% CI**	**p**	**n**	**HR**	**95% CI**	**p**
Age at ICI initiation	≤ 68	88	ref.			88	ref.		
	> 68	122	0.907	0.649-1.269	0.569	122	0.711	0.521-0.970	**0.032**
Sex	Male	146	ref.			146	ref.		
	Female	64	1.071	0.744-1.539	0.713	64	0.952	0.677-1.340	0.779
Tumor site	BC	172	ref.			172	ref.		
	UTUC	26	0.733	0.428-1.255	0.258	26	0.904	0.565-1.448	0.675
ICI drug	Atezo	76	ref.			76	ref.		
	Pembro	134	0.905	0.645-1.270	0.563	134	0.832	0.608-1.140	0.253
Setting	1L	84	ref.			84	ref.		
	2L	126	1.148	0.812-1.624	0.435	126	1.227	0.892-1.688	0.209
NAC	No	190	ref.			190	ref.		
	Yes	20	0.873	0.483-1.578	0.652	20	0.810	0.468-1.403	0.453
Radiochemotherapy	No	188	ref.			188	ref.		
	Yes	22	0.812	0.449-1.468	0.491	22	0.771	0.446-1.334	0.353
Radiotherapy	No	131	ref.			131	ref.		
	Yes	77	1.210	0.857-1.708	0.278	77	1.237	0.897-1.707	0.194
Radical surgery	No	118	ref.			118	ref.		
	Yes	92	0.659	0.468-.0929	**0.017**	92	0.768	0.562-1.051	0.099
ECOG PS	0	117	ref.			117	ref.		
	1+	82	1.902	1.347-2.686	**<0.001**	82	1.562	1.133-2.154	**0.007**
Liver metastasis	No	176	ref.			176	ref.		
	Yes	33	2.888	1.907-4.373	**<0.001**	33	2.588	1.725-3.883	**<0.001**
Visceral metastasis	No	114	ref.			114	ref.		
	Yes	95	1.559	1.117-2.176	**0.009**	95	1.366	1.003-1.859	**0.048**
Bone metastasis	No	161	ref.			161	ref.		
	Yes	49	2.160	1.485-3.141	**<0.001**	49	2.411	1.688-3.443	**<0.001**
LN-only metastasis	No	143	ref.			143	ref.		
	Yes	67	0.636	0.439-.0921	**0.017**	67	0.545	0.384-0.774	**<0.001**
Hemoglobin level	< 10 g/dl	48	ref.			48	ref.		
	≥ 10 g/dl	147	0.541	0.367-0.800	**0.002**	147	0.644	0.450-0.921	**0.016**
Bellmunt risk factors	0	74	ref.			74	ref.		
	1+	110	2.933	1.981-4.343	**<0.001**	110	2.213	1.561-3.137	**<0.001**
Bellmunt-CRP	0	33	ref.			33	ref.		
	1+	60	3.567	1.853-6.866	**<0.001**	60	2.244	1.326-3.795	**0.003**
CRP cutoff	< 30 mg/l	89	ref.			89	ref.		
	≥ 30 mg/l	15	1.876	0.993-3.543	0.052	15	1.627	0.895-2.956	0.110
NLR cutoff	< 5	109	ref.			109	ref.		
	≥ 5	47	1.883	1.230-2.882	**0.004**	47	2.170	1.476-3.191	**<0.001**
LDH cutoff	< 250 U/L	68	ref.			68	ref.		
	≥ 250 U/L	71	1.304	0.864-1.967	0.206	71	1.221	0.841-1.773	0.293
Albumin cutoff	< 35 g/l	27	ref.			27	ref.		
	≥ 35 g/l	102	0.418	0.256-0.683	**<0.001**	102	0.549	0.344-0.878	**0.012**
eGFR cutoff	< 40 ml/min	27	ref.			27	ref.		
	≥ 40 ml/min	111	0.514	0.309-0.857	**0.011**	111	0.756	0.471-1.215	0.249

Atezo: atezolizumab, Pembro: pembrolizumab, 1L: first-line, 2L: second-line, BC: bladder cancer, UTUC upper tract urothelial carcinoma, NAC: neoadjuvant chemotherapy, LN: lymph node

DOI:10.14753/SE.2025.3157

Table 7. Univariate Cox regression analysis for the first- and second-line cohorts. *Table 7 been published in the article: Váradi M. et al. Efficacy of immune checkpoint inhibitor therapy for advanced urothelial carcinoma in real-life clinical practice: results of a multicentric, retrospective study. Sci Rep. 2023 Oct 13;13(1):17378.* (115)

Variables		First-line setting								Second-line setting							
		Overall survival				Progression-free survival				Overall survival				Progression-free survival			
		n	HR	95% CI	p	n	HR	95% CI	p	n	HR	95% CI	p	n	HR	95% CI	p
Age at ICI initiation	≤ 68	26	ref.			26	ref.			62	ref.			62	ref.		
	> 68	58	0.857	0.476-1.540	0.605	58	0.755	0.438-1.303	0.313	64	0.983	0.649-1.488	0.934	64	0.714	0.484-1.054	0.090
Sex	Male	51	ref.			51	ref.			95	ref.			95	ref.		
	Female	33	1.008	0.568-1.787	0.979	33	0.949	0.561-1.606	0.845	31	1.185	0.735-1.909	0.486	31	1.047	0.661-1.658	0.844
ICI drug	Atezo	18	ref.			18	ref.			58	ref.			58	ref.		
	Pembro	66	0.554	0.293-1.049	0.070	66	0.577	0.320-1.041	0.068	68	1.099	0.723-1.669	0.659	68	1.047	0.710-1.545	0.816
Tumor site	BC	74	ref.			74	ref.			98	ref.			98	ref.		
	UTUC	6	1.509	0.460-4.949	0.497	6	1.686	0.667-4.266	0.270	20	0.623	0.338-1.148	0.129	20	0.710	0.408-1.234	0.224
NAC	No	77	ref.			77	ref.			113	ref.			113	ref.		
	Yes	7	1.971	0.824-4.714	0.127	7	1.731	0.738-4.063	0.207	13	0.548	0.239-1.256	0.155	13	0.527	0.255-1.088	0.083
Radiochemotherapy	No	66	ref.			66	ref.			122	ref.			122	ref.		
	Yes	18	0.561	0.263-1.198	0.135	18	0.628	0.318-1.239	0.179	4	3.994	1.430-11.152	**0.008**	4	2.242	0.813-6.185	0.119
Radiotherapy	No	45	ref.			45	ref.			86	ref.			86	ref.		
	Yes	38	1.122	0.638-1.973	0.689	38	1.066	0.637-1.784	0.807	39	1.341	0.863-2.086	0.192	39	1.500	0.985-2.283	0.059
Radical surgery	No	55	ref.			55	ref.			63	ref.			63	ref.		
	Yes	29	0.562	0.298-1.059	0.075	29	0.771	0.446-1.331	0.350	63	0.674	0.444-1.025	0.065	63	0.691	0.467-1.021	0.064
ECOG PS	0	39	ref.			39	ref.			78	ref.			78	ref.		
	1+	43	1.388	0.787-2.449	0.257	43	1.359	0.812-2.274	0.244	39	2.715	1.725-4.274	**<0.001**	39	1.941	1.265-2.980	**0.002**
Liver metastasis	No	74	ref.			74	ref.			102	ref.			102	ref.		
	Yes	9	1.720	0.766-3.864	0.189	9	1.529	0.721-3.240	0.268	24	3.624	2.213-5.937	**<0.001**	24	3.834	2.302-6.384	**<0.001**
Visceral metastasis	No	51	ref.			51	ref.			63	ref.			63	ref.		
	Yes	32	1.203	0.683-2.119	0.521	32	1.217	0.724-2.048	0.458	63	1.780	1.172-2.703	**0.007**	63	1.455	0.986-2.147	0.059
Bone metastasis	No	75	ref.			75	ref.			86	ref.			86	ref.		
	Yes	9	1.469	0.624-3.459	0.379	9	3.094	1.436-6.666	**0.004**	40	2.333	1.499-3.630	**<0.001**	40	2.187	1.440-3.323	**<0.001**
LN-only metastasis	No	55	ref.			55	ref.			88	ref.			88	ref.		
	Yes	29	1.094	0.613-1.951	0.761	29	0.686	0.394-1.194	0.182	38	0.459	0.280-0.750	**0.002**	38	0.469	0.289-0.740	**0.001**
Hemoglobin level	< 10 g/dl	17	ref.			17	ref.			31	ref.			31	ref.		
	≥ 10 g/dl	56	0.805	0.393-1.648	0.552	56	0.694	0.374-1.289	0.247	91	0.437	0.273-0.697	**0.001**	91	0.619	0.399-0.962	**0.033**
Bellmunt risk factors	0	19	ref.			19	ref.			55	ref.			55	ref.		
	1+	52	1.634	0.780-3.426	0.193	52	1.845	0.945-3.603	0.073	58	4.672	2.872-7.601	**<0.001**	58	2.924	1.897-4.508	**<0.001**
Bellmunt-CRP	0	10	ref.			10	ref.			23	ref.			23	ref.		
	1+	29	1.972	0.566-6.872	0.287	29	2.013	0.755-5.368	0.162	31	5.639	2.580-12.326	**<0.001**	31	2.823	1.486-5.362	**0.002**
CRP cutoff	< 30 mg/l	37	ref.			37	ref.			52	ref.			52	ref.		
	≥ 30 mg/l	4	1.029	0.230-4.606	0.970	4	2.079	0.619-6.978	0.236	11	2.057	0.998-4.240	0.051	11	1.402	0.700-2.805	0.340
NLR cutoff	< 5	34	ref.			34	ref.			75	ref.			75	ref.		
	≥ 5	19	1.923	0.905-4.086	0.089	19	2.909	1.460-5.794	**0.002**	28	1.802	1.073-3.026	**0.026**	28	1.851	1.155-2.965	**0.010**
LDH cutoff	< 250 U/L	31	ref.			31	ref.			37	ref.			37	ref.		
	≥ 250 U/L	23	1.405	0.683-2.890	0.356	23	1.422	0.750-2.694	0.281	48	1.234	0.744-2.045	0.415	48	1.088	0.685-1.729	0.721
Albumin cutoff	< 35 g/l	6	ref.			6	ref.			21	ref.			21	ref.		
	≥ 35 g/l	39	1.047	0.307-3.578	0.941	39	0.986	0.341-2.855	0.979	63	0.316	0.180-0.556	**<0.001**	63	0.436	0.254-0.747	**0.003**
eGFR cutoff	< 40 ml/min	15	ref.			15	ref.			12	ref.			12	ref.		
	≥ 40 ml/min	36	0.850	0.368-1.960	0.702	36	1.111	0.528-2.336	0.781	75	0.322	0.168-0.619	**0.001**	75	0.493	0.263-0.925	**0.028**

Atezo: atezolizumab, Pembro: pembrolizumab, 1L: first-line, 2L: second-line, BC: bladder cancer, UTUC upper tract urothelial carcinoma, NAC: neoadjuvant chemotherapy, LN: lymph node

Table 8. Multivariate Cox regression analysis (whole cohort).
Table 8 has been published in the article: Váradi M. et al. Efficacy of immune checkpoint inhibitor therapy for advanced urothelial carcinoma in real-life clinical practice: results of a multicentric, retrospective study. Sci Rep. 2023 Oct 13;13(1):17378. (115)

Varibles		Overall survival				Progression-free survival			
		n	HR	95% CI	p	n	HR	95% CI	p
Model 1									
ECOG PS	0	108	ref.			108	ref.		
	1+	76	1.909	1.304-2.795	**<0.001**	76	1.454	1.020-2.074	**0.039**
Visceral metastasis	No	104	ref.			104	ref.		
	Yes	80	1.812	1.085-3.025	**0.023**	80	1.109	0.725-1.697	0.633
Radical surgery	No	99	ref.			99	ref.		
	Yes	85	0.721	0.491-1.058	0.095	85	0.823	0.582-1.164	0.271
Bone metastasis	No	140	ref.			140	ref.		
	Yes	44	2.327	1.446-3.743	**<0.001**	44	2.017	1.315-3.095	**0.001**
LN-only metastasis	No	123	ref.			123	ref.		
	Yes	61	1.564	0.858-2.854	0.145	61	0.798	0.479-1.328	0.385
Hemoglobin level	< 10 g/dl	46	ref.			46	ref.		
	≥ 10 g/dl	138	0.651	0.425-0.997	**0.048**	138	0.750	0.507-1.110	0.151
Model 2									
Bellmunt risk factors	0	74	ref.			74	ref.		
	1+	110	2.638	1.762-3.949	**<0.001**	110	2.017	1.408-2.891	**<0.001**
Radical surgery	No	99	ref.			99	ref.		
	Yes	85	0.741	0.509-1.080	0.119	85	0.888	0.630-1.252	0.499
Bone metastasis	No	140	ref.			140	ref.		
	Yes	44	1.978	1.278-3.060	**0.002**	44	2.001	1.331-3.008	**<0.001**
LN-only metastasis	No	123	ref.			123	ref.		
	Yes	61	1.051	0.683-1.618	0.821	61	0.759	0.509-1.132	0.176

4.1.4. Determinants of treatment response and disease control

Information on response during ICI therapy was available for a subset of patients (n=181). Among the clinical parameters, age at ICI initiation, ECOG PS, the presence of liver, bone, or LN metastases, and Bellmunt risk factors showed significant associations with response and disease control. Additionally, two laboratory parameters, NLR and albumin level, also showed a significant association with these outcomes. The results are summarized in Table 9 and 10.

Table 9. Association between the radiographic response, disease control and different clinicopathological variables (whole cohort). *Table 9 has been published in the article: Váradi M. et al. Efficacy of immune checkpoint inhibitor therapy for advanced urothelial carcinoma in real-life clinical practice: results of a multicentric, retrospective study. Sci Rep. 2023 Oct 13;13(1):17378.* (115)

			Disease control			Response		
Variables		**All patients n (%)**	**PD n (%)**	**SD/PR/ CR n (%)**	**p**	**PD/SD n (%)**	**PR/CR n (%)**	**p**
Sex	Male	124 (69)	46 (37)	78 (63)		77 (60)	47 (40)	
	Female	57 (31)	23 (40)	34 (60)	0.675	38 (67)	19 (33)	0.553
Age at ICI	≤68 years	74 (41)	37 (50)	37 (50)		57 (77)	17 (23)	
	>68 years	107 (59)	32 (30)	75 (70)	**0.006**	58 (54)	49 (46)	**0.002**
Drug	Atezo	64 (35)	28 (44)	36 (56)		41 (64)	23 (36)	
	Pembro	117 (65)	41 (35)	76 (65)	0.249	74 (63)	43 (37)	0.913
ICI setting	1L	73 (40)	25 (34)	48 (66)		49 (67)	24 (33)	
	2L	108 (60)	44 (41)	64 (59)	0.378	66 (61)	42 (39)	0.41
Tumor site	BC	148 (86)	58 (39)	90 (61)		97 (66)	51 (34)	
	UTUC	24 (14)	9 (38)	15 (62)	0.875	13 (54)	11 (46)	0.282
Radical surgery	Yes	84 (46)	29 (35)	55 (65)		48 (57)	36 (43)	
	No	97 (54)	40 (41)	57 (59)	0.354	67 (69)	30 (31)	0.096
Radiochemotherapy	No	160 (88)	62 (39)	98 (63)		100 (63)	60 (37)	
	Yes	21 (12)	7 (33)	14 (67)	0.631	15 (71)	6 (29)	0.424
Bellmunt risk factors	0	72 (43)	17(23)	55 (77)		35 (48)	37 (52)	
	1+	95 (57)	45 (47)	50 (53)	**0.002**	70 (74)	25 (26)	**0.001**
Bellmunt-CRP	0	33 (39)	9 (27)	24 (73)		16 (49)	17 (51)	
	1+	52 (61)	28 (54)	24 (46)	**0.016**	40 (77)	12 (23)	**0.007**
ECOG PS	0	104 (60)	31 (30)	73 (70)		57 (55)	47 (45)	
	1+	69 (40)	33 (48)	36 (52)	**0.016**	52 (75)	17 (25)	**0.006**
Liver metastasis	No	158 (87)	54 (34)	104 (66)		98 (62)	60 (38)	
	Yes	23 (13)	15 (65)	8 (35)	**0.004**	17 (74)	6 (26)	0.268
Visceral metastasis	No	103 (57)	37 (36)	66 (64)		69 (67)	34 (33)	
	Yes	78 (43)	32 (41)	46 (59)	0.484	46 (59)	32 (41)	0.267
LN-only metastasis	No	121 (67)	55 (45)	66 (55)		80 (66)	41 (34)	
	Yes	60 (33)	14 (23)	46 (77)	**0.004**	35 (58)	25 (42)	0.306
Bone metastasis	No	140 (77)	41 (29)	99 (71)		82 (59)	58 (41)	
	Yes	41 (23)	28 (68)	13 (32)	**<0.001**	33 (80)	8 (20)	**0.010**
CRP	<30 mg/l	80 (86)	33 (41)	47 (59)		51 (64)	29 (36)	
	≥ 30mg/l	13 (14)	9 (69)	4 (31)	0.060	11 (85)	2 (15)	0.139
LDH	<250 U/L	62 (49)	22 (35)	40 (65)		38 (61)	24 (39)	
	≥250 U/L	65 (51)	28 (43)	37 (57)	0.381	44 (68)	21 (32)	0.451
NLR	<5	102 (70)	31 (30)	71 (70)		55 (54)	47 (46)	
	≥5	43 (30)	22 (51)	21 (49)	**0.018**	34 (79)	9 (21)	**0.005**
Hemoglobin	<10 g/dl	41 (23)	20 (49)	21 (51)		31 (76)	10 (24)	
	≥10 g/dl	134 (77)	47 (35)	87 (65)	0.114	80 (60)	54 (40)	0.064
Albumin	<35 g/l	23 (19)	12 (52)	11 (48)		21 (91)	2 (9)	
	≥35 g/l	98 (81)	29 (30)	69(70)	**0.039**	53 (54)	45 (46)	**0.001**
eGFR	<40 ml/min	25 (20)	12 (48)	13 (52)		18 (72)	7 (28)	
	≥40 ml/min	97 (80)	35 (36)	62 (64)	0.275	55 (57)	42 (43)	0.164

Table 10. Association between the radiographic response, disease control and different clinicopathological variables for first- and second-line settings. *Table 10 has been published in the article: Váradi M. et al. Efficacy of immune checkpoint inhibitor therapy for advanced urothelial carcinoma in real-life clinical practice: results of a multicentric, retrospective study. Sci Rep. 2023 Oct 13;13(1):17378.* (115)

		First-line setting							Second-line setting						
			Disease control			Response				Disease control				Response		
Variables		**All patients**	**PD**	**SD/PR/CR**		**PD/SD**	**PR/CR**		**All patients**	**PD**	**SD/PR/CR**		**PD/SD**	**PR/CR**	
		n (%)	**n (%)**	**n (%)**	**p**	**n (%)**	**n (%)**	**p**	**n (%)**	**n (%)**	**n (%)**	**p**	**n (%)**	**n (%)**	**p**
Sex	Male	44 (60)	14 (32)	30 (68)	0.590	27 (61)	17 (39)	0.197	80 (74)	32 (40)	48 (60)	0.791	50 (63)	30 (37)	0.617
	Female	29 (40)	11 (38)	18 (62)		22 (76)	7 (24)		28 (26)	12 (43)	16 (57)		16 (57)	12 (43)	
Age at ICI	≤68 years	21 (29)	9 (43)	12 (57)	0.325	17 (81)	4 (19)	0.110	53 (49)	28 (53)	25 (47)	**0.012**	40 (75)	13 (25)	**0.003**
	>68 years	52 (71)	16 (31)	36 (69)		32 (62)	20 (38)		55 (51)	16 (29)	39 (71)		26 (47)	29 (53)	
Drug	Atezo	16 (22)	8 (50)	8 (50)	0.133	13 (81)	3 (19)	0.173	48 (44)	20 (42)	28 (58)	0.861	28 (58)	20 (42)	0.596
	Pembro	57 (78)	17 (30)	40 (70)		36 (63)	21 (37)		60 (56)	24 (40)	36 (60)		38 (63)	22 (37)	
Tumor site	BC	63 (91)	21 (33)	42 (67)	0.413	42 (67)	21 (33)	0.403	85 (83)	37 (44)	48 (56)	0.426	55 (65)	30 (35)	0.109
	UTUC	6 (9)	3 (50)	3 (50)		5 (83)	1 (17)		18 (17)	6 (33)	12 (67)		8 (44)	10 (56)	
Radical surgery	Yes	29 (40)	10 (34)	19 (66)	0.972	17 (59)	12 (41)	0.209	55 (51)	19 (35)	36 (65)	0.182	31 (56)	24 (44)	0.303
	No	44 (60)	15 (34)	29 (66)		32 (73)	12 (27)		53 (49)	25 (47)	28 (53)		35 (66)	18 (34)	
Radiochemotherapy	No	56 (77)	19 (34)	37 (66)	0.917	37 (66)	19 (34)	0.728	104 (96)	43 (41)	61 (57)	0.514	63 (61)	41 (39)	0.561
	Yes	17 (23)	6 (35)	11 (65)		12 (71)	5 (29)		4 (4)	1 (25)	3 (75)		3 (75)	1 (25)	
Bellmunt risk factors	0	19 (29)	4 (21)	15 (79)	0.100	11 (58)	8 (42)	0.185	53 (52)	13 (25)	40 (75)	**0.004**	24 (45)	29 (55)	**0.005**
	1+	47 (71)	20 (43)	27 (57)		35 (74)	12 (26)		48 (48)	25 (52)	23 (48)		35 (73)	13 (27)	
Bellmunt-CRP	0	10 (28)	3 (30)	7 (70)	0.379	6 (60)	4 (40)	0.310	23 (47)	6 (26)	17 (74)	**0.013**	10 (43)	13 (57)	**0.016**
	1+	26 (72)	12 (46)	14 (54)		20 (77)	6 (23)		26 (53)	16 (62)	10 (38)		20 (77)	6 (23)	
ECOG PS	0	32 (45)	8 (25)	24 (75)	0.103	18 (56)	14 (44)	**0.035**	72 (71)	23 (32)	49 (68)	**0.043**	39 (54)	33 (46)	0.139
	1+	39 (55)	17 (44)	22 (56)		31 (79)	8 (21)		30 (29)	16 (53)	14 (47)		21 (70)	9 (30)	
Liver metastasis	No	66 (90)	22 (33)	44 (67)	0.614	46 (70)	20 (30)	0.151	92 (85)	32 (35)	60 (65)	**0.003**	52 (57)	40 (43)	**0.019**
	Yes	7 (10)	3 (43)	4 (57)		3 (43)	4 (57)		16 (15)	12 (75)	4 (25)		14 (88)	2 (12)	
Visceral metastasis	No	46 (63)	14 (30)	32 (70)	0.370	32 (70)	14 (30)	0.526	57 (53)	23 (40)	34 (60)	0.931	37 (65)	20 (35)	0.392
	Yes	27 (37)	11 (41)	16 (59)		17 (63)	10 (37)		51 (47)	21 (41)	30 (59)		29 (57)	22 (43)	
LN-only metastasis	No	47 (64)	20 (43)	27 (57)	**0.044**	32 (68)	15 (32)	0.055	74 (69)	35 (47)	39 (53)	**0.041**	48 (65)	26 (35)	0.238
	Yes	26 (36)	5 (19)	21 (81)		17 (65)	9 (35)		34 (31)	9 (26)	25 (74)		18 (53)	16 (47)	
Bone metastasis	No	65 (89)	18 (28)	47 (72)	**<0.001**	42 (65)	23 (35)	0.194	75 (69)	23 (31)	52 (69)	**0.001**	40 (53)	35 (47)	0.012
	Yes	8 (11)	7 (88)	1 (12)		7 (88)	1 (12)		33 (31)	21 (64)	12 (36)		26 (79)	7 (21)	
CRP	<30 mg/l	34 (89)	12 (35)	22 (65)	0.124	22 (65)	12 (35)	0.151	46 (84)	21 (46)	25 (54)	0.249	29 (63)	17 (37)	0.395
	≥ 30mg/l	4 (11)	3 (75)	1 (25)		4 (100)	0 (0)		9 (16)	6 (67)	3 (33)		7 (78)	2 (22)	
LDH	<250 U/L	28 (56)	8 (29)	20 (71)	0.217	19 (68)	9 (32)	0.981	34 (44)	14 (41)	20 (59)	0.925	19 (56)	15 (44)	0.299
	≥250 U/L	22 (44)	10 (45)	12 (55)		15 (68)	7 (32)		43 (56)	18 (42)	25 (58)		29 (67)	14 (33)	
NLR	<5	32 (64)	7 (22)	25 (68)	**0.006**	18 (56)	14 (44)	**0.018**	80 (76)	24 (30)	46 (70)	0.747	37 (46)	33 (54)	0.096
	≥5	18 (36)	11 (61)	7 (39)		16 (89)	2 (11)		25 (24)	11 (44)	14 (56)		18 (72)	7 (28)	
Hemoglobin	<10 g/dl	15 (22)	5 (33)	10 (67)	0.857	11 (73)	4 (27)	0.594	26 (24)	15 (58)	11 (42)	**0.036**	20 (77)	6 (23)	**0.052**
	≥10 g/dl	53 (78)	19 (36)	34 (64)		35 (66)	18 (34)		81 (76)	28 (35)	53 (65)		45 (56)	36 (44)	
Albumin	<35 g/l	6 (14)	2 (33)	4 (67)	0.932	6 (100)	0 (0)	0.058	17 (22)	10 (59)	7 (41)	**0.020**	15 (88)	2 (12)	**0.005**
	≥35 g/l	38 (86)	12 (32)	26 (68)		23 (61)	15 (39)		60 (78)	17 (28)	43 (72)		30 (50)	30 (50)	
eGFR	<40 ml/min	15 (32)	5 (33)	10 (67)	0.632	11 (73)	4 (27)	0.465	10 (13)	7 (70)	3 (30)	**0.029**	7 (70)	3 (30)	0.338
	≥40 ml/min	32 (68)	13 (41)	19 (59)		20 (63)	12 (37)		65 (87)	22 (34)	43 (66)		35 (54)	30 (46)	

Atezo: atezolizumab, Pembro: pembrolizumab, 1L: first-line, 2L: second-line, BC: bladder cancer, UTUC upper tract urothelial carcinoma

4.1.5. Comparison of the real-world cohort with corresponding clinical trial cohorts

Although the multicenter design of this study enabled the inclusion of a diverse group of patients reflective of real-world clinical practice, the characteristics of our cohort—such as age, sex, and primary tumor location—were largely comparable to those reported in the corresponding clinical trials (KEYNOTE-045, KEYNOTE-052, IMvigor211, and IMvigor210), with only minor differences. Interestingly, our real-world cohort included a lower rate of liver metastases, an unexpected finding given that investigators often tend to select more fit patients for inclusion in clinical trials.

The ORRs observed in our study were similar to those reported in the clinical trials, with the exception of second-line atezolizumab treatment. In this setting, the ORR of the real-

life cohort (34.5%) was more than 20% higher compared to the respective clinical trials (14.5% and 13.3% in IMvigor210/cohort 2 and IMvigor211, respectively).

The median OS time for our entire cohort was 13.6 months. When patients were grouped by the administered drugs and treatment settings, the poorest OS was observed in the first-line atezolizumab-treated subgroup, although the case numbers in this group were low. A notable OS difference was seen in the second-line atezolizumab-treated groups, with the real-life cohort showing a median OS of 17.0 months, compared to 7.9 and 11.1 months reported in IMvigor210/cohort 2 and IMvigor211, respectively (Table 11)

Table 11. Comparison of the present real-world cohort with patient cohorts in the corresponding clinical trials. *Table 11 has been published in the article: Váradi M. et al. Efficacy of immune checkpoint inhibitor therapy for advanced urothelial carcinoma in real-life clinical practice: results of a multicentric, retrospective study. Sci Rep. 2023 Oct 13;13(1):17378.* (115)

	Pembrolizumab				**Atezolizumab**				
	First-line		**Second-line**		**First-line**		**Second-line**		
Variables	**Real-world cohort n=66**	**KEYNOTE-052 n=370**	**Real-world cohort n=68**	**KEYNOTE-045 n=270**	**Real-world cohort n=18**	**IMvigor210 Cohort 1 n=119**	**Real-world cohort n=58**	**IMvigor210 Cohort 2 n=310**	**IMvigor 211 n=467**
Age at ICI initiation, years median	72	74	68	67	72	73	68	66	67
Sex									
Male, no (%)	41 (62.1)	286 (77.3)	55 (80.9)	200 (74.1)	10 (55.6)	96 (87.3)	40 (69.0)	241 (77.7)	110 (23.6)
Female, no (%)	25 (37.9)	84 (22.7)	13 (19.1)	70 (25.9)	8 (44.4)	23 (20.9)	18 (31.0)	69 (22.3)	357 (76.4)
Location of primary tumor									
UTUC, no (%)	6 (9.1)	69 (18.6)	9 (13.2)	38 (14.1)	0	33 (30.0)	11 (19.0)	65 (21.0)	126 (27.0)
BC, no (%)	58 (87.9)	300 (81.1)	54 (79.4)	232 (85.9)	16 (88.9)	85 (77.3)	44 (75.9)	230 (74.2)	324 (69.4)
Boths, no (%)	2 (3.0)	0 (0.0)	5 (7.4)	0 (0.0)	2 (11.1)		3 (5.2)		
ECOG-PS at ICI initiation									
0, no(%)	36 (54.5)	80 (21.6)	39 (57.4)	119 (44.1)	3 (16.7)		39 (67.2)	117 (37.7)	218 (46.7)
1, no (%)	19 (28.8)	133 (35.9)	15 (22.1)	143 (53.0)	9 (50.0)		15 (25.9)	193 (62.3)	249 (53.3)
2, no (%)	9 (13.6)	156 (42.2)	6 (8.8)	2 (0.7)	6 (33.3)	24 (21.8)	1 (1.7)		
3, no (%)	0 (0.0)	1 (0.3)	1 (1.5)	0 (0.0)	0 (0.0)		1 (1.7)		
NA, no (%)	2 (3.0)	0 (0.0)	7 (10.3)	6 (2.2)	0 (0.0)		2 (3.4)		
Liver metastasis, no (%)	7 (10.6)	78 (21.1)	14 (20.6)	91 (33.7)	2 (11.1)	25 (21.0)	10 (17.2)	96 (31.0)	138 (29.6)
ORR, no (%)	21 (31.8)	106 (28.6)	22 (32.4)	57 (21.1)	3 (16.7)	27 (22.7)	20 (34.5)	45 (14.5)	62 (13.3)
DCR, % (95% CI)	40 (60.6)	173 (46.8)	36 (52.9)	104 (38.5)	8 (44.4)	56 (47.1)	28 (48.3)	104 (33.5)	154 (33.0)
Best overall response									
CR, no (%)	8 (12.1)	33 (8.9)	4 (5.9)	25 (9.3)	0 (0.0)	11 (9.2)	1 (1.7)	15 (4.8)	16 (3.4)
PR, no (%)	13 (19.7)	73 (19.7)	18 (26.5)	32 (11.99	3 (16.7)	16 (13.4)	19 (32.8)	30 (9.7)	46 (9.9)
SD, no (%)	19 (28.8)	67 (18.1)	14 (20.6)	47 (17.4)	5 (27.8)	29 (24.4)	8 (13.8)	59 (19.0)	92 (19.7)
PD, no (%)	17 (25.8)	157 (42.4)	24 (35.3)	131 (48.5)	8 (44.4)	43 (36.1)	20 (34.5)	159 (51.3)	240 (51.4)
NA, no (%)	9 (13.6)	40 (10.8)	8 (11.8)	35 (13.0)	2 (11.1)	20 (16.8)	10 (17.2)	47 (15.2)	73 (15.6)
PFS, months, median	8.1	2.0	3.6	2.1	2.0	2.7	6.4	2.1	2.1
Death, no (%)	37 (56.1)	239 (64.6)	46 (67.6)	208 (77.0)	13 (72.2)	59 (49.6)	44 (75.9)	193 (62.3)	324 (69.4)
OS, months, median	15.6	11.3	8.8	10.3	5.6	15.9	17.0	7.9	11.1

ICI: immune checkpoint inhibitor, BC: bladder cancer, UTUC: upper tract urinary cancer, ORR: overall response rate, DCR: disease control rate, CR: complete response, PR: partial response, SD: stable disease, PD: progressive disease, NA: not available, PFS: progression-free survival, OS: overall survival

4.2. Gene expression analysis

4.2.1. Cohort description and follow-up details

The patient cohort included in the gene expression analysis consisted of 100 UC patients. A comprehensive description of the patient characteristics for the entire cohort, as well as for first- and second-line treatment groups, is provided in Table 12. Among patients, 34 received atezolizumab and 66 received pembrolizumab. The median age at therapy initiation was 70.3 years (range: 30.9–88.8 years). Bellmunt risk scores could be calculated for 97% of the patients, and data on PD-L1 IHC positivity were available in 77 cases.

The median follow-up from ICI therapy baseline was 12.0 months. Of the 99 patients with available radiographic response could be evaluated, three experienced complete remission (CR), and 31 had a partial response (PR), resulting in an ORR of 34%. Disease

Table 12. Patient characteristics for the whole cohort and by treatment lines

		Whole cohort	Fist-line	Second-line
Variables		**n (%)**	**n (%)**	**n (%)**
Total number of patients		100	30	70
Age at ICI initiation, years median [range]		70.3 [30.9-88.8]	72.1 [46.8-88.4]	68.8 [30.9-88.8]
Sex	Male	73 (73)	19 (63)	54 (77)
	Female	27 (27)	11 (37)	16 (23)
Location of primary tumor	UTUC	14 (14)	3 (10)	11 (16)
	BC	79 (79)	25 (83)	54 (77)
	Both	7 (7)	2 (7)	5 (7)
Setting	1L	30 (30)	30 (100)	0 (0)
	2L	70 (70)	0 (0)	70 (100)
Drug	Atezolizumab	34 (34)	8 (27)	26 (37)
	Pembrolizumab	66 (66)	22 (73)	44 (63)
ECOG-PS at ICI initiation	0	56 (56)	16 (53)	40 (57)
	1	33 (33)	12 (40)	21 (30)
	2	9 (9)	2 (7)	7 (10)
	NA	2 (2)	0 (0)	2 (3)
Matastatic sites	Only LN	29 (29)	10 (33)	19 (27)
	Liver	17 (17)	2 (7)	15 (21)
	Visceral	51 (51)	14 (47)	37 (53)
	Bone	24 (24)	2 (7)	22 (31)
Bellmunt risk factors	0	40 (40)	11 (37)	29 (41)
	1	43 (43)	15 (50)	28 (40)
	2-3	14 (14)	3 (10)	11 (16)
	NA	3 (3)	1 (3)	2 (3)
PD-L1 IHC	CPS>10	46 (46)	14 (47)	32 (46)
	CPS<10	31 (31)	8 (27)	23 (33)
	NA	23 (23)	8 (27)	15 (21)

ICI: immune checkpoint inhibitor, UTUC: upper tract urothelial carcinoma, BC: bladder cancer, 1L: first-line, 2L: second-line, NAC: neoadjuvant chemotherapy, LN: lymph node, PD-L1: programmed death-ligand 1, IHC: immunohistochemistry, CPS: combined positive score

control was achieved in 58 patients. The median PFS was 4.9 months (95% CI: 3.4–8.6). During the follow-up, 75 patients passed away, and the median OS was 13.6 months (95% CI: 9.1–18.4) (Table 13).

Table 13. Follow-up characteristics for the whole cohort and by treatment lines

	Whole cohort	**Fist-line**	**Second-line**
Variables	**n (%)**	**n (%)**	**n (%)**
Time of follow-up, months, median [range]	12.0 [0.5-81.9]	12.8 [0.5-81.9]	11.7 [0.5-58.3]
Best overall response			
Complete response (CR)	3 (3)	3 (10)	0
Partial response (PR)	31 (31)	6 (21)	25 (36)
Stable disease (SD)	24 (24)	7 (24)	17 (24)
Progressive disease (PD)	41 (41)	13 (45)	28 (40)
No radiologic evaluation performed	1	1	0
ORR	34 (34)	9 (31)	25 (36)
DCR	58 (58)	16 (55)	42 (60)
PFS, months, median [95% CI]	4.9 [3.4-8.6]	6.5 [2.9-13.8]	4.6 [3.1-8.6]
Death at last follow-up	75 (75)	22 (73)	53 (76)
OS, months, median [95% CI]	13.6 [9.1-18.4]	13.7 [8.7-30.9]	12.2 [7.6- 23.4]

ORR: overall response rate, DCR: disease control rate, PFS: progression-free survival, OS: overall survival, CI: confidence interval

4.2.2. Clinicopathological factors associated with survival or therapy response

As there were significant overlaps between the real-life cohort described previously and the gene expression analysis cohort, the results of the statistical analyses for the gene expression cohort, including Cox regression and Chi-squared tests, were similar to those presented in previous chapters. A summary of results is presented in Table 14.

Table 14. Univariate Cox regression analysis (OS, PFS), and association between the ORR, DCR and different clinicopathological variables.

		OS				PFS				DCR			ORR		
Variables		**n**	**HR**	**95% CI**	**p**	**n**	**HR**	**95% CI**	**p**	**No (n)**	**Yes (n)**	**p**	**No (n)**	**Yes (n)**	**p**
Age at ICI start	≤ 68	44	ref.			44	ref.			23	21		31	13	
	> 68	56	0.822	0.522-1.294	0.398	56	0.934	0.600-1.454	0.761	18	37	**0.050**	34	21	0.369
Sex	Male	73	ref.			73	ref.			29	43		48	24	
	Female	27	1.126	0.676-1.875	0.650	27	1.430	0.886-2.308	0.143	12	15	0.708	17	10	0.730
Tumor site	BC	79	ref.			79	ref.			35	43		55	23	
	UTUC	14	1.068	0.526-2.167	0.856	14	1.013	0.534-1.923	0.968	4	10	0.256	6	8	**0.044**
ICI drug	Atezolizumab	34	ref.			34	ref.			14	19		18	15	
	Pembrolizumab	66	0.989	0.619-1.579	0.963	66	1.003	0.636-1.580	0.991	27	39	0.885	47	19	0.100
Setting	1L	30	ref.			30	ref.			13	16		20	9	
	2L	70	1.017	0.618-1.675	0.947	70	1.027	0.636-1.658	0.913	28	42	0.657	45	25	0.655
ECOG PS	0	56	ref.			56	ref.			20	36		32	24	
	1+	42	1.616	1.013-2.579	**0.044**	42	1.282	0.821-2.003	0.274	20	21	0.197	31	10	0.060
Liver met	No	83	ref.			83	ref.			30	52		52	30	
	Yes	17	2.369	1.336-4.201	**0.003**	17	2.289	1.295-4.045	**0.004**	11	6	**0.032**	13	4	0.302
Visceral met	No	49	ref.			49	ref.			18	31		33	16	
	Yes	51	1.323	0.837-2.091	0.232	51	1.143	0.736-1.775	0.551	23	27	0.349	32	18	0.726
Bone met	No	76	ref.			76	ref.			24	51		44	31	
	Yes	24	2.140	1.271-3.604	**0.004**	24	1.486	0.893-2.471	0.127	17	7	**0.001**	21	3	**0.010**
LN-only met	No	71	ref.			71	ref.			33	37		47	23	
	Yes	29	0.661	0.391-1.116	0.121	29	0.770	0.467-1.269	0.305	8	21	0.072	18	11	0.628
Baseline Hg	<10 g/dl	21	ref.			21	ref.			13	8		18	3	
	≥10 g/dl	72	0.426	0.246-0.737	**0.002**	72	0.491	0.291-0.828	**0.008**	25	46	0.029	43	28	**0.032**
Bellmunt score	0	40	ref.			40	ref.			10	30		19	21	
	1+	57	1.936	1.192-4.144	**0.008**	57	1.696	1.066-2.699	**0.026**	29	27	0.008	43	13	**0.003**
Baseline CRP	<30 mg/l	45	ref.			45	ref.			17	27		30	14	
	≥30 mg/l	11	1.402	0.654-3.005	0.386	11	1.060	0.488-2.299	0.884	8	3	**0.042**	9	2	0.373
Baseline NLR	<5	54	ref.			54	ref.			21	33		30	24	
	≥5	31	1.376	0.821-2.304	0.226	31	1.241	0.758-2.033	0.391	15	15	0.324	24	6	**0.025**
Baseline LDH	<250 U/L	32	ref.			32	ref.			12	19		21	10	
	≥250 U/L	31	2.735	1.499-4.988	**0.001**	31	2.215	1.266-3.872	**0.005**	16	15	0.307	23	8	0.576
Baseline albumin	<35 g/l	17	ref.			17	ref.			8	9		14	3	
	≥35 g/l	45	0.924	0.441-1.934	0.833	45	0.523	0.274-0.996	**0.049**	13	31	0.197	24	20	**0.045**
Baseline eGFR	<40 ml/min	17	ref.			17	ref.			11	6		13	4	
	≥40 ml/min	53	0.397	0.211-0.749	**0.004**	53	0.648	0.356-1.182	0.157	22	30	0.109	33	19	0.323

OS: overall survival, PFS: progression-free survival, DCR: disease control rate, ORR: overall response rate, CI: confidence interval, ICI: immune checkpoint inhibitor, UTUC: upper tract urothelial carcinoma, BC: bladder cancer, 1L: first-line, 2L: second-line, ECOG-PS: Eastern Cooperative Oncology Group performance status, LN: lymph node, Hg: hemoglobin, NLR: neutrophil-to-lymphocyte ratio, LDH: lactate dehydrogenase

4.2.3. Differential gene expression and survival

In total, 95 genes were associated with OS (Figure 7). Of these, 23 genes remained significant after false discovery rate (FDR) correction (Table 15). Subsequent validation using the KM Plotter online tool in the transcriptome dataset from the IMvigor210 study

DOI:10.14753/SE.2025.3157

(second-line atezolizumab in over 300 mUC patients) confirmed the prognostic value of 6 genes (Table 15).

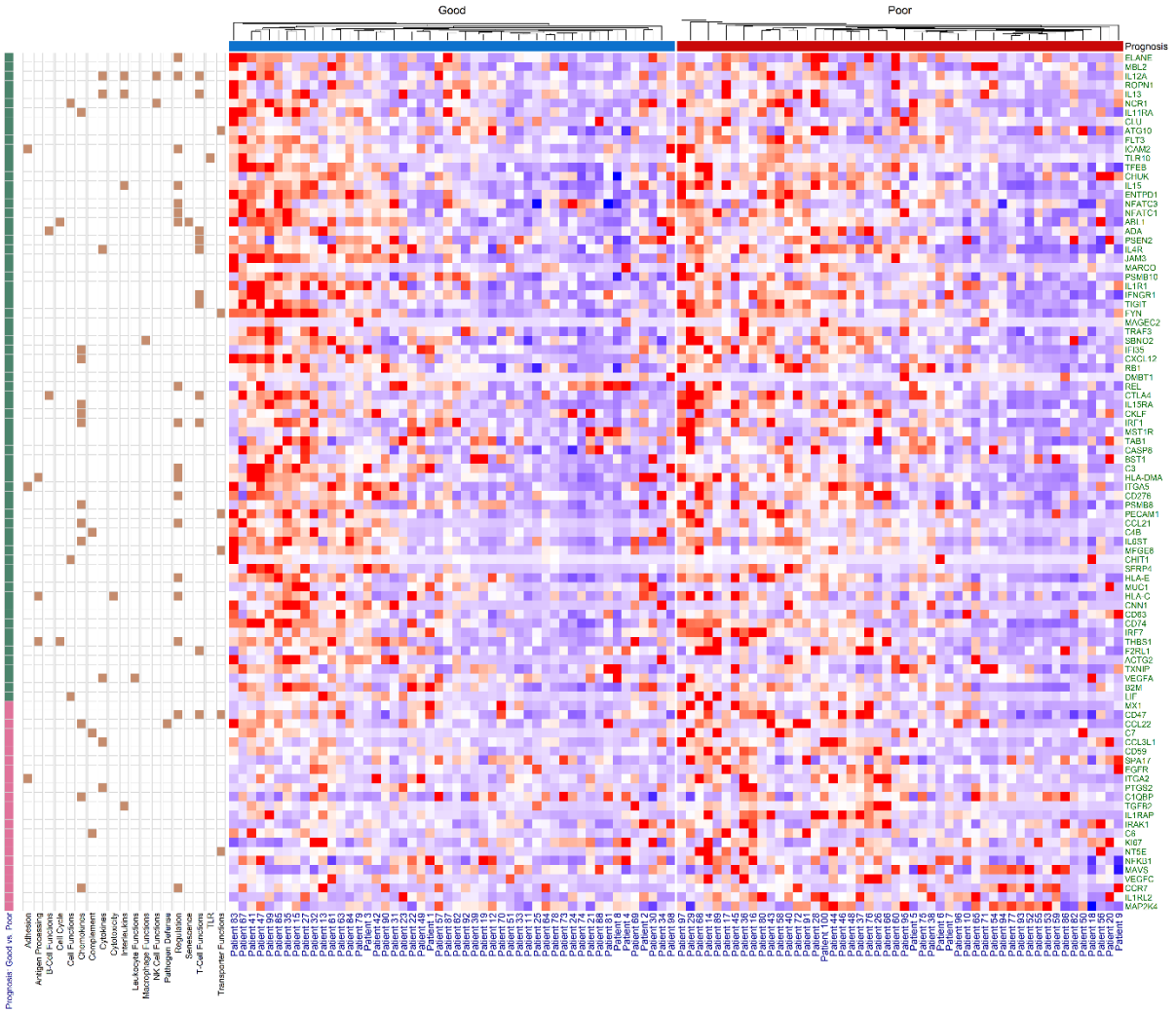

Figure 7. Heatmap of differentially expressed genes between good (>12 months) and poor (<12 months) OS. The green and pink boxes on the left represent protective (up-regulated) and risk (down-regulated) genes, respectively. The brown boxes indicate cancer-immunity cycle enrichment annotation information.(Own figure)

Table 15. List of genes with significant (FDR-corrected) prognostic value and their immune response category according to NanoString® annotation

Gene name	FDR	HR	95% CI	Cut-off value	Immune Response Category (Nanostring® Annotation)
MAP2K4 [#]	0.003	2.37	1.47-3.83	268	Innate immune response
IL4R	0.004	0.43	0.25-0.72	570	Cytokines, T-Cell Functions
C3	0.007	0.39	0.23-0.67	1624	Innate immune response, Regulation
CXCL12 [#]	0.012	0.45	0.27-0.76	656	Chemokines
ICAM2	0.016	0.42	0.26-0.69	126	Adhesion, Regulation
IRF7* [#]	0.016	0.49	0.30-0.78	324	Innate immune response
MFGE8	0.018	0.41	0.23-0.73	2125	Transporter Functions
ROPN1	0.019	0.55	0.33-0.93	10	-
ELANE	0.019	0.54	0.32-0.83	2	Regulation
C1QBP	0.019	2.44	1.35-4.40	1118	Chemokines
RB1	0.020	0.52	0.32-0.86	610	-
CD63	0.021	0.47	0.28-0.78	15453	-
NCR1* [#]	0.021	0.55	0.32-0.74	12	Cell Functions, NK Cell Functions
CHUK	0.025	0.51	0.28-0.78	388	Innate immune response
MBL2 [#]	0.028	0.57	0.35-0.92	10	Innate immune response
PSMB8* [#]	0.029	0.47	0.28-0.78	850	Chemokines
IL4	0.030	0.71	0.45-1.12	4	Interleukins, Regulation, T-Cell Functions
CR2*	0.035	0.64	0.40-1.02	18	Innate immune response, B-Cell Functions
DMBT1	0.037	0.55	0.32-0.88	7	Innate immune response
PSMB10* [#]	0.041	0.48	0.29-0.79	727	Humoral immune response
IL12A [#]	0.043	0.56	0.34-0.87	8	Adaptive immune response, Cytokines, Interleukins, NK Cell Functions, Regulation, T-Cell Functions
ENTPD1	0.046	0.53	0.31-0.85	257	Adaptive immune response
HLA-E* [#]	0.047	0.51	0.30-0.85	3343	Regulation

* validated in IMvigor210 transcriptome dataset

[#] validated in KM Plotter pan-cancer dataset

4.2.4. Differential gene expression and therapy response

The Wilcoxon test identified 20 genes (analyzed as continuous variables) significantly associated with ORR. Genes linked to good ORR included *MAGEA12, SPP1, GPI, ENO2, TFRC, BST1, C3, MME, MAGEA3, PRAME, NFKBIA*, and *CTAG1B*, while those associated with poor ORR included *TMEFF2, FLT4, ABCB1, CCL24, CREBBP*, *CD209*, *C8G*, and *MYD88.* Furthermore, 43 genes were associated with disease control (DCR)

DOI:10.14753/SE.2025.3157

(Figure 8A). Validation using the ROC Plotter online tool in the pan-cancer dataset revealed 16 differentially expressed genes (Figure 9). Among these, *IRF1* and *PSMB10* also exhibited significantly different expression levels in the validation UC cohort from the transcriptome dataset of IMvigor210. Notably, *PSMB10* was the only gene validated for both endpoints: DCR and OS (Figure 10).

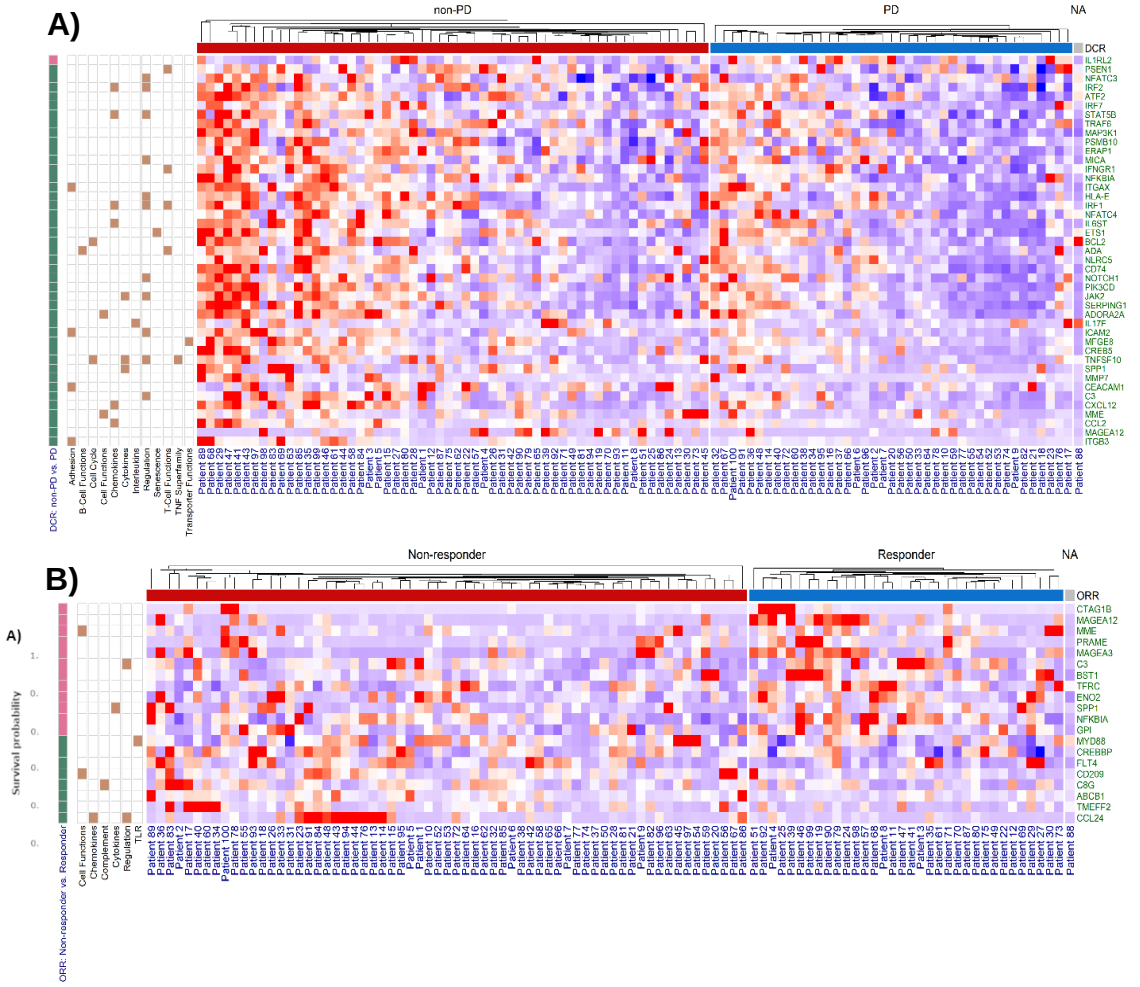

Figure 8. Heatmap of differentially expressed genes between responder and non-responder groups according to A) DCR and B) ORR. The green and pink boxes on the left represent up-regulated and down-regulated genes, respectively. The brown boxes indicate cancer-immunity cycle enrichment annotation information. (Own figure)

DOI:10.14753/SE.2025.3157

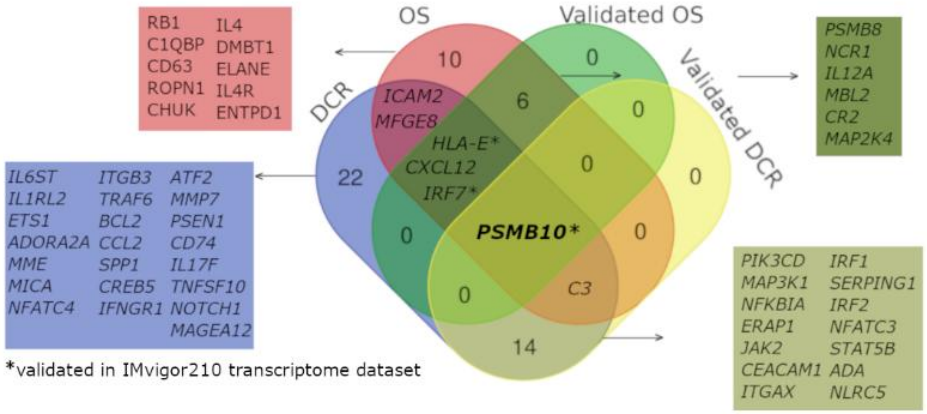

Figure 9. Venn diagram illustrating overlapping associations of genes with different endpoints.

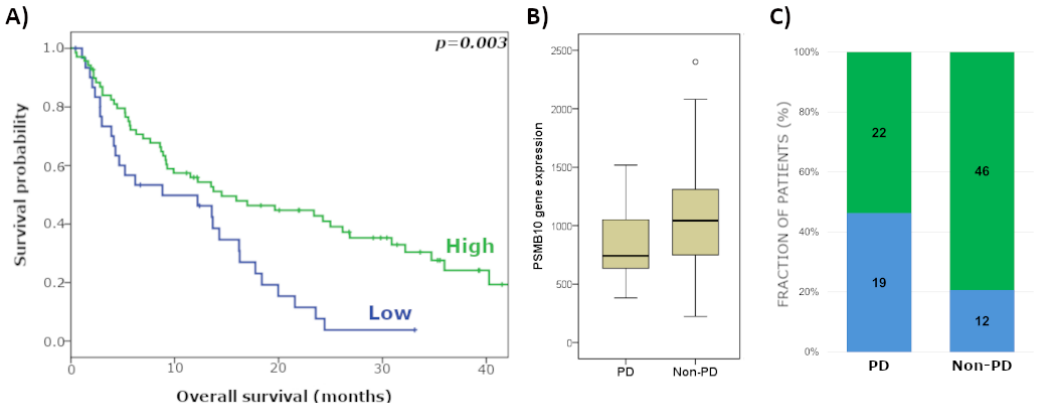

Figure 10. Survival (A) and therapy response (boxplots (B) and bar charts (C)) based on gene expression levels of PSMB10. Blue bars represent low gene expression, and green bars represent high gene expression. (Own figure)

4.2.5. Correlation of molecular subtypes with survival and therapy response

We identified molecular subtypes using four different classification systems (MDA, TCGA, Lund, and consensus). No significant differences were observed in OS or PFS among the consensus and Lund-classification subgroups (p=0.575 for OS and p=0.441 for PFS in both systems) (Figure 11A and C). However, patients in the MDA-p53-like subgroup demonstrated significantly longer OS (p=0.024) and PFS (p=0.043) compared to those in the luminal and basal subgroups (Figure 11D). According to the TCGA classification system, the luminal subgroup showed inferior OS (p=0.023) and PFS (p=0.038) compared to other groups. Additionally, the neuronal and luminal-infiltrated

DOI:10.14753/SE.2025.3157

subtypes exhibited longer OS, though the number of cases in the neuronal group was limited (Figure 11B).

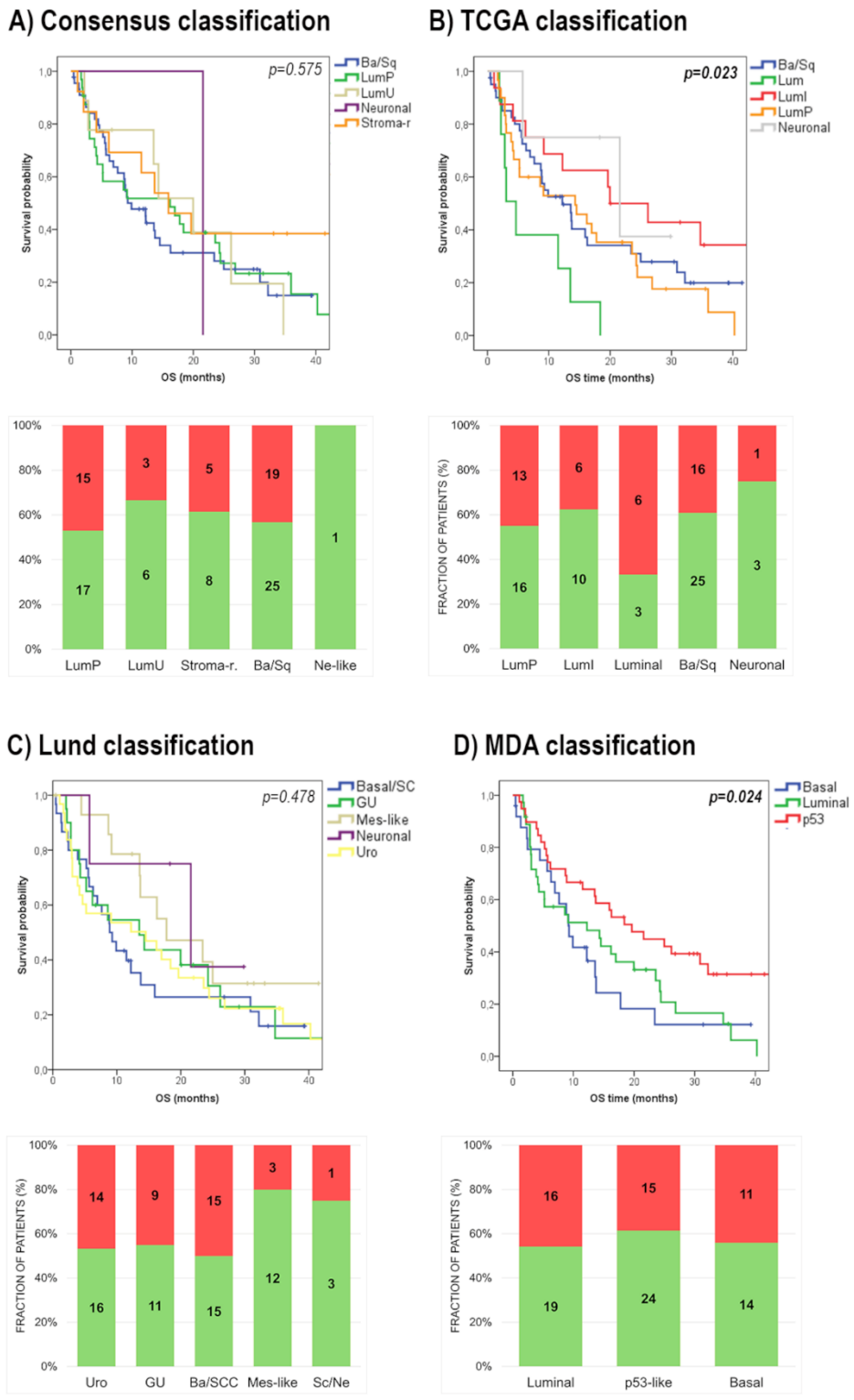

Figure 11. Survival and radiographic response of different molecular subtypes. Radiographic response is indicated as green for non-progressive disease (non-PD) and red for progressive disease (PD). Subtypes are shown based on the (A) consensus, (B) TCGA, (C) Lund, and (D) MDA classification systems. (Own figure)

Among the evaluated signature scores (Table 3), high neuronal scores (≥3.2), calculated from the expression levels of 10 genes — *APLP1, CHGB, ENO2, GNG4, MSI1, PEG10, PLEKHG4B, RND2, SV2A,* and *TUBB2B* — were associated with improved OS and PFS (Figure 12)

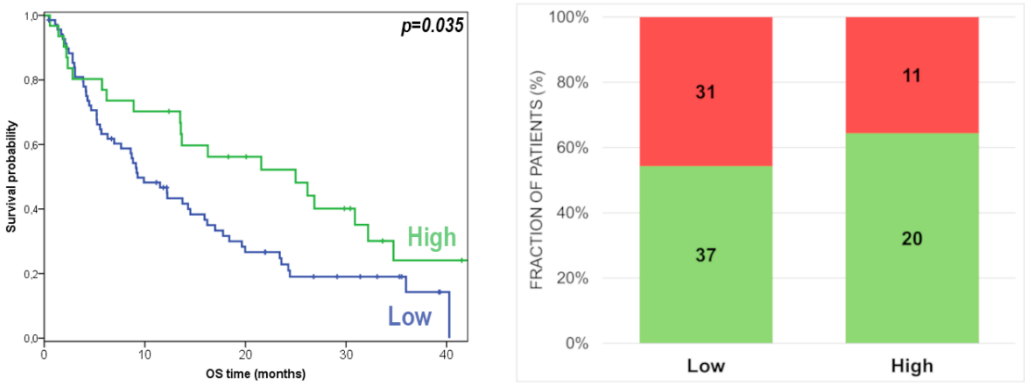

Figure 12. Survival and radiographic response of patients with low (<3.2) versus high (>3.2) neuronal signature score. Radiographic response is indicated as green for non-progressive disease (non-PD) and red for progressive disease (PD). (Own figure)

4.2.6. Combined model of clinicopathological and gene expression data

We used the Random Survival Forest model to identify the best prognostic model combining clinicopathological and molecular factors that showed significant associations with OS in univariate analysis. An additional inclusion criteria was the availability of the given parameter for at least 80% of the patients in order to avoid a small sample sizes. We randomized our dataset into a training subcohort (75%) to develop the prediction algorithm and a test subcohort (25%), to evaluate the trained classifier. We calculated both the area under the receiver operating characteristic (ROC) curves (AUC) and the concordance index (C-index) for the developed predictions. Our final model included four laboratory parameters (LDH, Hg, eGFR, NLR) and 10 gene-expression based markers (*CR2, HLA-E, IRF7, PSMB10, PSMB8, CXCL12, IL12A, MAP2K4, IRF1*, Neuronal signature score). The AUC and the C-index of this prediction were 0.89 and 0.77 on the test set, respectively (Figure 13A-B). Each patient was assigned a score based on this prediction model, and using the median score (38.5), patients could be divided into low-score and high-score groups. The median overall survival (OS) of the high-score group

DOI:10.14753/SE.2025.3157

was inferior to that of the low-score group (7.6 months *vs.* 40.3 months, HR=10.86, p=0.002) (Figure 13C).

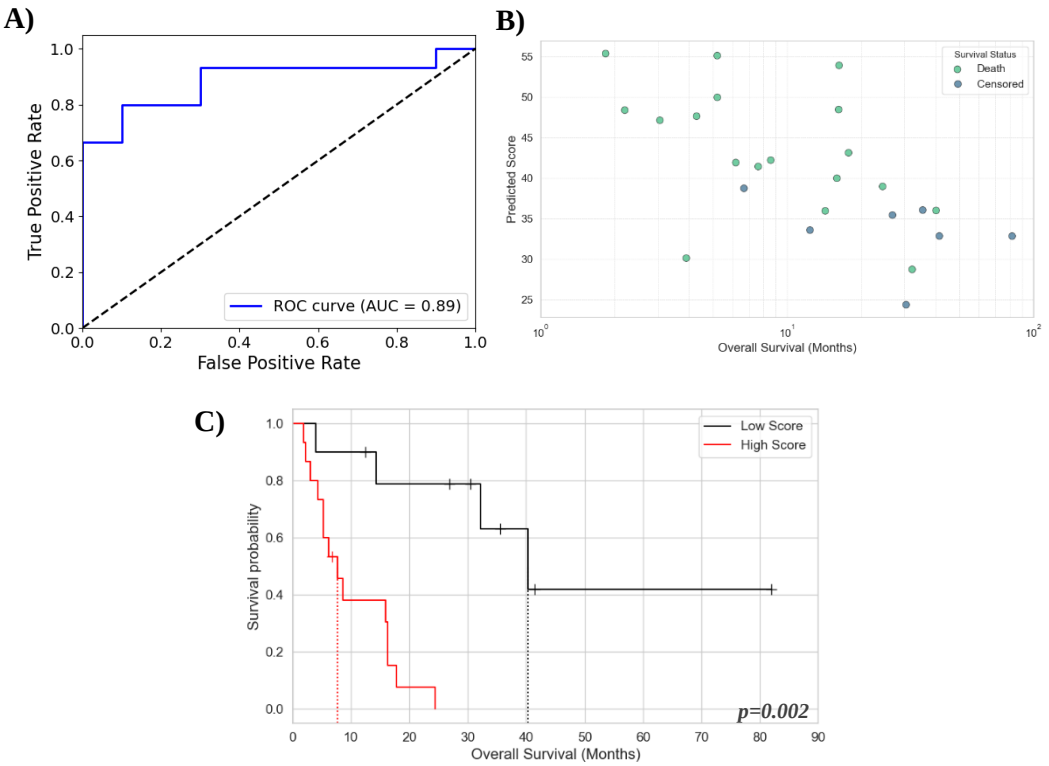

Figure 13. The best combination model's performance and survival analysis: ROC Curve (A), Survival *vs.* score scatter plot (B) and Kaplan-Meier plot (C) (Own figure)

4.3. Soluble PD-L1 concentration in serum samples

4.3.1. Cohort description and follow-up details

Serum samples before ICI initiation (baseline) were available from 10 male and 2 female UC patients. Only one patient was treated with pembrolizumab, all of the others received atezolizumab therapy (Table 16). The median of the baseline sPD-L1 concentration was 90.0 pg/ml (range: 25.3-169.0). On-treatment serum samples, collected before the second immunotherapy cycle, were available for 11 patients with a median sPD-L1 concentration of 2316.0 pg/ml (range: 42.5-3818.6). Eight cycles (range: 2-47) was the median therapy lengths. The median follow-up was 39.7 months (range: 2.2-63.6) with seven patients died within this period.

Table 16. Patients' characteristics and serum PD-L1 concentrations

		Number of patients	**sPD-L1 cc. median (range) [pg/ml]**
Variables		**n (%)**	**Baseline**
Age at ICI initiation	≤ 68	5 (41.7)	74.6 (26.9-169.0)
	> 68	7 (58.3)	95.2 (25.3-145.0)
Sex	Male	10 (83.3)	94.2 (60.0 -169.0)
	Female	2 (16.7)	26.1 (25.3-26.9)
Setting	1L	2 (16.7)	87.1 (80.9-93.3)
	2L	10 (83.3)	90.9 (25.3-169.0)
Drug	Atezolizumab	11 (91.7)	93.3 (25.3-169.0)
	Pembrolizumab	1 (8.3)	26.9 (-)
ECOG PS	0	8 (66.7)	84.0 (25.3-99.8)
	1+	4 (33.3)	115.8 (80.9-169.0)
Only LN met	No	9 (75.0)	86.6 (25.3-169.0)
	Yes	3 (25.0)	95.2 (26.9-99.8)

1L: first-line, 2L: second-line, LN: lymph node

DOI:10.14753/SE.2025.3157

4.3.2. Correlation of serum PD-L1 concentrations with survival

Although the limited number of cases did not allow for a valid statistical analysis, higher pre-treatment serum PD-L1 concentrations were associated with poor OS in Kaplan-Meier analysis dichotomized at the median (p=0.069) (Figure 14A).

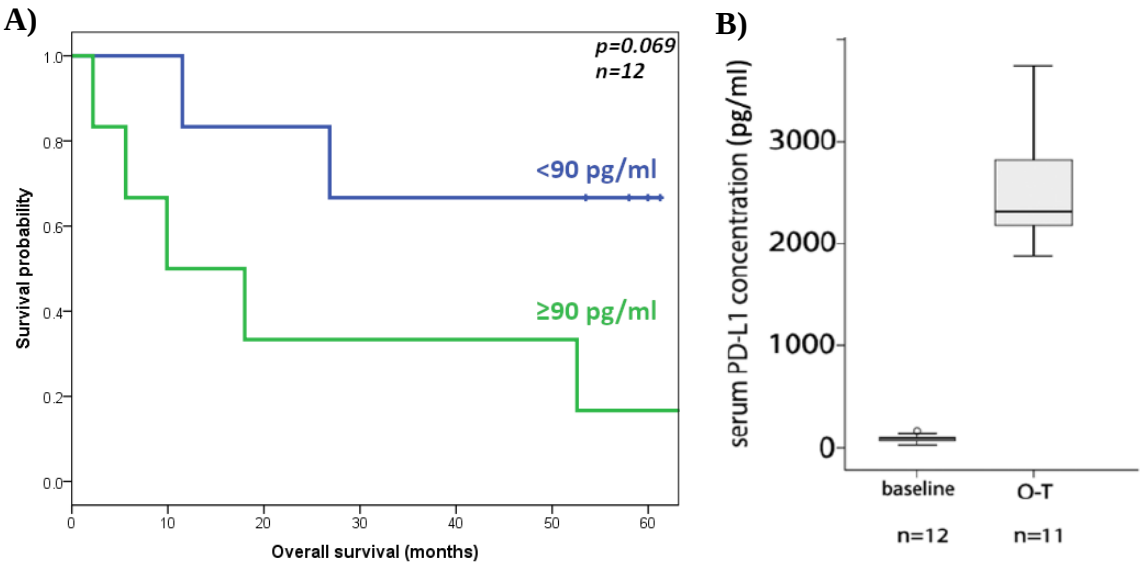

Figure 14. Overall survival stratified by pre-treatment sPD-L1 levels in ICI-treated patients (A) and box-plot presentation of serum PD-L1 levels in baseline and on-treatment (O-T) samples (collected at 2-3. therapy cycles (B) (116)

Figure 14 has been published in the article: Krafft U. et al. High Serum PD-L1 Levels Are Associated with Poor Survival in Urothelial Cancer Patients Treated with Chemotherapy and Immune Checkpoint Inhibitor Therapy. Cancers (Basel). 2021 May 22;13(11):2548.

4.3.3. Serum PD-L1 level changes during ICI therapy

Interestingly, a >25-fold increase could be observed in sPD-L1 concentrations in all on-treatment samples after atezolizumab treatment (Figure 14B), whereas no such increase was showed in the samples of the pembrolizumab-treated patient. To rule out a possible interference between the therapeutic antibody, atezolizumab and the ELISA kit, we performed an ELISA analysis with atezolizumab solution, which showed no positive reaction in our ELISA assay. This suggests no interference between the therapeutic anti-PD-L1 antibody and the antibodies used in the ELISA.

5. Discussion

The aim of the present work was to assess the characteristics of UC patients receiving ICI treatment in real-world clinical practice, compare the efficacy of two widely used ICI drugs (pembrolizumab and atezolizumab) with respective clinical trial results, and evaluate the prognostic and predictive value of standard clinicopathological and laboratory parameters. Through molecular analyses, we intended to identify potential ICI-predictive genes in UC patients, examine whether different molecular subtypes show different therapy response and/or survival, and to evaluate the prognostic value of sPD-L1 as a serum biomarker.

The introduction of ICIs has significantly changed the treatment paradigm for mUC. While prospective clinical trials have shown, that these agents can provide durable therapeutic effects and prolong survival, only a relatively small subgroup of patients benefits from this therapy (31, 32, 35, 73-75). Due to their strict eligibility criteria, clinical trials often include highly selected patient cohorts, that do not broadly represent real-world populations (76, 77). Therefore, real-world data have become more important to researchers and regulators recently, as they provide insights into the effectiveness of medical interventions in a broader and more representative patient population (78). In addition, the therapeutic landscape of advanced UC continues to expand, highlighting the growing importance of accurate prediction of the ICI therapy-efficacy. Since standalone biomarkers display limited predictive and/or prognostic value, integrative approaches that combine various clinicopathological, laboratory, and molecular factors are essential to improve predictive accuracy.

Although the multicentric nature of our study allowed the inclusion of a broad range of patients in real clinical practice, the characteristics of our cohort (age, sex location of primary tumor) were comparable to those of the respective clinical trials with only few exception (Table 11). Interestingly, our real-world cohort included a lower rate of patients with liver metastasis, which is rather an unexpected finding given that investigators often prefer to include fitter patients in clinical trials. Similarly, liver metastatic patients were underrepresented in a Danish real-world pembrolizumab-treated UC cohort. In the present study, the presence of liver metastasis - a well-known risk-factor of OS and cancer-specific survival – was associated with poor OS. In line with these findings, a meta-analysis has reported a significant association between the presence of visceral or

liver metastasis and worse OS in pembrolizumab-treated UC patients (79, 80). Due to shorter life expectancy, these patients often do not receive systemic treatment, which may explain their underrepresentation in the real-world cohort. Additionally, some oncologists in real-world practice may choose cisplatin-based chemotherapy or prioritize enrolling these patients in clinical trials, such as those involving antibody-drug conjugates, which were actively recruiting during the study period.

The ORRs in this study were comparable to those reported in the respective clinical trials, except for second-line atezolizumab treatment, where the real-world cohort showed a notably higher ORR (34.5%) compared to IMvigor210/cohort 2 (14.5%) and IMvigor211 (13.3%). This is supported by similar findings from other real-world studies, such as Tural *et al.*'s study of a Turkish atezolizumab-treated UC population (28.7%) (81). Additionally, DCRs were higher, in the real-world population compared to clinical trials.

The median OS for the entire cohort was 13.6 months, with the worst OS observed in first-line atezolizumab-treated patients, although subgroup size was small. Second-line atezolizumab-treated patients in the real-world cohort had a median OS of 17.0 months, significantly longer than reported in the respective clinical trials (7.9 and 11.1 months for IMvigor210/cohort 2 and IMvigor211, respectively). Similar findings from other real-world studies suggest greater benefits of atezolizumab in real-world conditions than observed in clinical trials (81-83).

In this study, worse ECOG performance status, metastases (visceral, liver, or bone), low hemoglobin, and Bellmunt risk factors were independent predictors of shorter OS.

ECOG status is a validated prognostic parameter in oncology outpatient settings. It has been shown to be an independent prognostic factor for OS in advanced UC treated with platinum-containing regimens (67). ECOG is also an important factor for the determination of "platinum-ineligible" patients, and thus worse ECOG status can also be a criterion of the administration of ICI drugs in the first-line setting (84). Impaired ECOG status has been shown to correlate with shorter OS and worse ORR in metastatic melanoma, head and neck carcinoma, and non-small cell lung cancer (85-87). According to our findings, impaired ECOG performance status was significantly associated with shorter OS and worse radiographic response in our ICI-treated UC cohort. These results align with previous studies reporting worse OS for UC patients with poor ECOG status, particularly those with ECOG PS≥2 in both first- and second-line ICI therapy settings

(79, 81, 88). Based on these, ICIs appear to be less effective in patients with poor ECOG status. This effect may be a simple prognostic association, but ECOG was shown to be linked to immunocompetence in cancer patients. A previous study suggested that T-lymphocyte subpopulations (CD8+/CD4+ T cells) reflect ECOG PS in gastric cancer patients (89), which suggests also a functional association between ICI efficacy and ECOG status.

The Bellmunt risk stratification is a further well-established prognostic model in mUC (32). Although initially developed for chemotherapy cohorts, it was shown to be associated with prognosis of ICI-treated patients. To improve its predictive accuracy in ICI-treated UC patients, an enhanced version, the Bellmunt-CRP score, was recently introduced by Abuhelwa *et al.* (66). In this study, we evaluated the performance of this enhanced score using real-world data and we could confirm its improved prognostic value in an independent patient cohort for the first time.

Among haematological biomarkers, elevated pre-treatment NLR and low albumin levels are significantly associated with worse OS, PFS, and therapy response in various cancers, including UC (90-93). Elevated NLR can result from either increased neutrophil abundance or decreased lymphocyte levels. Neutrophils may promote a pro-tumor microenvironment by releasing immunosuppressive factors (*e.g.* reactive oxygen species, vascular endothelial growth factor and matrix metalloproteinase 9) (94), while low lymphocyte levels can reduce tumor-infiltrating lymphocytes, leading to a weaker anti-tumor response (95). Our results confirm that NLR is a promising candidate for a cost-effective and widely accessible biomarker for ICI treated UC patients.

Interestingly, our results suggested advanced age (>68 years) to be associated with enhanced DCR, PFS, but not OS. In accordance, Kugel *et al.* reported that melanoma patients over the age of 60 showed a higher response rate to anti-PD-1 therapy and these findings could be confirmed by *in vivo* experiments, showing significantly increased response to anti-PD-1 in aged mice. Furthermore, they found a significantly higher population of regulatory T cells (Tregs) in young mice, skewing the CD8+:Treg ratio (96). These findings suggest that the increased sensitivity in elderly patients could be a consequence of the accumulation of CD8+ T cells, which are the primary target cell type of anti-PD1 checkpoint blockade. Some other studies, however, found that cytotoxic CD8+ T cells, which are the primary target cell type of immune checkpoint blockade, in

elderly adults have decreased T cell receptor (TCR) diversity, reduced proliferative capacity, and increased sensitivity to apoptotic signals, that contribute to a diminished anti-tumoral immunogenic response (97, 98). On the contrary, expression of PD-1 was found to be increased on the T cells of elderly adults, although its blockade did not restore T cell activity to the same extent as in younger adults (99). The meta-analysis of Elias *et al.* found no differences in the OS and PFS between younger and older ICI-treated patients with metastatic solid tumors (100). These conflicting results suggest that age as prognostic factor in ICI therapy may have a cancer-specific role, and highlight the need for further research before considering age as a factor in determining ICI therapy response.

Although our clinical data analysis revealed that several clinicopathological and laboratory parameters correlate with OS or radiographic response, their therapy-specific prognostic or predictive potential is limited, as they mainly reflect the stage of progression, tumor burden and the general condition of the patients, but do not account for the biology of the tumor. The molecular heterogeneity of the tumor and the composition of its microenvironment can play a key role in individual sensitivity to ICI therapy, making the identification of biomarkers that account for these characteristics crucial. Therefore, we conducted a detailed molecular characterization of 100 UC tumor samples, investigating the gene expression profiles of more than 700 immune-related and 48 molecular subtype-specific genes.

Our gene expression analysis identified 23 genes with prognostic value for OS, and six of these could be validated in a large independent UC cohort (IMvigor210 study transcriptome dataset). According to ORR and DCR 20 and 43 genes showed significantly different expressions, respectively. Although 7 genes (*C3, CXCL12, HLA-E, ICAM2, IRF7, MFGE8, PSMB10*) were associated with both endpoints (OS and DCR), *PSMB10* was the only one validated in the IMvigor210 transcriptome data for both outcomes.

The *PSMB10* (Proteasome Subunit Beta Type 10) gene encodes a component of the immunoproteasome (IP), a specialized proteasome involved in antigen processing. The IP is predominantly expressed in immune cells, such as antigen-presenting cells and plays a critical role in the generation of peptide fragments presented by MHC class I molecules to cytotoxic T cells (101). Recent studies in various cancer types have shown that

overexpression of IP subunits (PSMB8, PSMB9, PSMB10) is associated with improved survival and better response to ICI therapies (102-104). Wang *et al.* demonstrated that the transcript levels of *PSMB8, PSMB9, PSMB10, PSME1, PSME2* and *IRF1* are closely associated with CD8+ T lymphocyte levels in UC (105). Additionally, they developed a predictive score (IP-score) based on these six genes to assess clinical response to ICI therapy. Notably, UC patients who responded to atezolizumab therapy exhibited a high IP-score compared to non-responders, and immune checkpoint genes, such as PD-1/PD-L1, were overexpressed in the high IP-score group (106). Our results further validate the predictive value of IP-related genes (*PSMB8, PSMB10* and *IRF1*).

In this study, we applied various molecular subtype classification systems (MDA, TCGA, Lund, Consensus) with an independently validated gene-panel-based approach and found the highest ORR and longest OS in the neuronal, TCGA-luminal infiltrated, Lund-mesenchymal, and MDA-p53-like subtypes. However, some associations lacked statistical significance due to small case numbers in less common subtypes. Our finding that the TCGA-luminal infiltrated subtype responds well to ICI therapy aligns with literature data linking it to high immune/stromal infiltration and elevated PD-L1 expression (61, 62). Previous studies suggested that tumors with a neuronal (neuroendocrine-like) subtype exhibit exceptionally favorable responses to ICI therapies. However, the low case numbers, possibly due to strict inclusion criteria, limit the robustness of these findings (63, 64). To address this issue, we analyzed neuronal signature scores and found high scores (≥3.2) associated with improved OS and PFS. This indicates that even patients with non-neuronal subtypes but elevated neuronal scores may benefit from ICI therapy.

Recently, integrative prognostic models combining clinicopathological, laboratory, molecular, and genetic factors have gained interest for improving therapeutic decision-making. Some risk stratification models incorporating clinicopathological and laboratory factors such as ECOG PS, liver metastasis, platelet count, NLR, and LDH *etc.* outperformed the Bellmunt model (88, 107, 108). Additionally, a 3-factor model incorporating a genetic factor (TMB) identified patients with low NLR, no visceral metastases, and high TMB as treatment responders (93). In the present work, we developed a combination model that includes laboratory and gene expression-based factors, which enhanced the prognostic performance of standalone biomarkers.

According to our results, patients with high-risk scores showed significantly worse OS compared to those in the low-risk score group. These findings need to be further validated in independent ICI-treated UC cohorts.

The prognostic role of the soluble form of PD-L1 in ICI-treated cohorts is a subjective of active research. Esophageal and renal cell cancer patients with elevated pre-treatment sPD-L1 levels showed better outcomes following ICI therapy, while in NSCLC and melanoma an opposite tendency could be observed (52, 109-111). The results of a recent meta-analysis on the predictive value of the pre-treatment sPD-L1 for ICI inhibitor therapy confirm the tumor-type dependent nature of this potential biomarker (112). In the present study, we found that higher pre-treatment sPD-L1 concentrations were associated with poor OS in ICI-treated UC patients; however, the low number of cases limits the strength of this finding. In addition, we observed a significant sPD-L1 flare in on-treatment serum samples from atezolizumab-treated but not pembrolizumab-treated patients. The therapy-specific nature of this phenomenon has been observed in other studies, where only PD-L1, not PD-1 inhibitors, induced an sPD-L1 increase (113, 114). The exact mechanism behind this sPD-L1 flare-up remains unclear and its clinical relevance requires further investigation.

DOI:10.14753/SE.2025.3157

6. Conclusion

This study investigated the efficacy of ICI therapy for UC in real-world clinical practice, finding atezolizumab and pembrolizumab effective for advanced or metastatic UC patients, regardless of treatment line, with second-line atezolizumab showing better outcomes than respective clinical trials. The study emphasized the need for easily accessible prognostic and predictive markers, such as clinicopathological and laboratory parameters, to optimize treatment decisions. Key prognostic factors included ECOG PS, metastasis sites, NLR, hemoglobin, albumin, and eGFR levels. The Bellmunt risk score's utility could be confirmed, and its performance could be further improved by adding CRP to the model. Our study provides valuable real-world insights, highlighting key similarities and differences compared to approval studies. These findings can inform larger meta-analyses and contribute to high-level clinical conclusions, helping to position ICI therapy within the complex treatment landscape of mUC.

In addition, we analyzed the expression of over 700 immune-related genes to identify potential ICI-predictive biomarkers in our institutional UC patient cohort. We found 23 genes with significant prognostic value and 43 genes significantly associated with DCR. Validation in a large, independent transcriptome dataset of ICI-treated UC patients confirmed the prognostic and predictive significance of *PSMB10*.

We used a novel gene-panel-based approach to classify the tumor tissue samples into molecular subtypes according to four various classification systems and assessed the predictive value of molecular subtype classification in the context of ICI therapy. We identified the highest ORR and OS in TCGA-luminal infiltrated, Lund-mesenchymal, and MDA p53-like subtypes. Although neuronal subtypes showed promising ICI responses, small case numbers limited statistical robustness. Analyzing neuronal signature scores revealed that high scores correlated with improved OS and PFS, suggesting that even non-neuronal subtypes with elevated neuronal signature scores may benefit from ICI therapy.

By combining different laboratory and gene expression-based parameters, we developed a prognostic model, the applicability of which needs to be evaluated in other ICI-treated UC cohorts or within the framework of a prospective study, in order to help to optimize therapeutic decision-making in the future.

DOI:10.14753/SE.2025.3157

Finally, we evaluated the prognostic value of the serum biomarker sPD-L1 and found that higher pre-treatment serum PD-L1 levels are associated with poor OS in ICI-treated UC patients, although the small sample size limits the strength of this finding.

Our study identified a series of clinicopathological, laboratory, serum, and gene expression-based markers that could help to optimize the disease management of UC, pending validation in prospective clinical studies.

DOI:10.14753/SE.2025.3157

7. Summary

In recent years, ICIs have become available for the systemic treatment of advanced UC. PD-1 and PD-L1 inhibitor therapies have resulted in durable therapeutic effect in a subset of patients. The molecular background of the large individual heterogeneity regarding the response to ICIs is still poorly understood.

The aim of my research was to identify factors affecting ICI therapy effectiveness in a real-world UC cohort. We assessed the clinical characteristics of more than 200 UC patients receiving ICI treatment in routine clinical settings and compared the effectiveness of pembrolizumab and atezolizumab against results from respective clinical trials. Our findings revealed that the ORRs and OS times were comparable to those reported in the clinical trials. Moreover, we identified worse ECOG PS, metastases, low hemoglobin, and Bellmunt risk factors as independent predictors of shorter OS.

The molecular part of this work aimed to identify potential ICI-predictive genes through gene expression analysis of the tumor using the NanoString technology. Our gene expression analysis identified 23 genes with prognostic value for OS. For ORR and DCR, 20 and 43 genes, respectively, showed significantly different expressions. Although seven genes were associated with both endpoints (OS and DCR), *PSMB10* was the only one validated in the IMvigor210 transcriptome data for both outcomes.

Additionally, we examined how different molecular subtypes of UC relate to therapy response and survival outcomes. Using various classifications, we found the highest ORR and longest OS in the neuronal, TCGA-luminal infiltrated, and MDA-p53-like subtypes. To address the limitation of small sample sizes, we analyzed neuronal signature scores and found high scores associated with improved OS and PFS. This indicates that even patients with non-neuronal subtypes but elevated neuronal scores may benefit from ICI therapy.

We applied the Random Survival Forest model to identify the best combination model incorporating clinicopathological and molecular factors. Our prognostic model effectively distinguished patients with longer survival on ICI therapy.

Finally, we evaluated the prognostic value of soluble PD-L1 for ICI-treated UC patients. Higher pre-treatment serum PD-L1 concentrations were associated with poor OS. In addition, we observed a significant sPD-L1 flare in on-treatment serum samples from atezolizumab-treated but not pembrolizumab-treated patients.

8. References

1. Siegel RL, Miller KD, Wagle NS, Jemal A. Cancer statistics, 2023. CA Cancer J Clin. 2023;73(1):17-48.
2. Bray F, Laversanne M, Sung H, Ferlay J, Siegel RL, Soerjomataram I, Jemal A. Global cancer statistics 2022: GLOBOCAN estimates of incidence and mortality worldwide for 36 cancers in 185 countries. CA Cancer J Clin. 2024;74(3):229-263.
3. Burger M, Catto JW, Dalbagni G, Grossman HB, Herr H, Karakiewicz P, Kassouf W, Kiemeney LA, La Vecchia C, Shariat S, Lotan Y. Epidemiology and risk factors of urothelial bladder cancer. Eur Urol. 2013;63(2):234-241.
4. Liu S, Yang T, Na R, Hu M, Zhang L, Fu Y, Jiang H, Ding Q. The impact of female gender on bladder cancer-specific death risk after radical cystectomy: a meta-analysis of 27,912 patients. Int Urol Nephrol. 2015;47(6):951-958.
5. Dahm P, Gschwend JE. Malignant non-urothelial neoplasms of the urinary bladder: a review. Eur Urol. 2003;44(6):672-681.
6. Kaufman DS, Shipley WU, Feldman AS. Bladder cancer. Lancet. 2009;374(9685):239-249.
7. Slusarczyk A, Zapala P, Zapala L, Borkowski T, Radziszewski P. Cancer-Specific Survival of Patients with Non-Muscle-Invasive Bladder Cancer: A Population-Based Analysis. Ann Surg Oncol. 2023;30(12):7892-7902.
8. Siegel RL, Miller KD, Jemal A. Cancer statistics, 2016. CA Cancer J Clin. 2016;66(1):7-30.
9. National Cancer Institute: Cancer Stat Facts: Bladder Cancer [Internet]. 2022 [Cited 2024 Dec 4]. Available from: https://seer.cancer.gov/statfacts/html/urinb.html.
10. Witjes J.A. HMB, A. Carrión, R. Cathomas,, E.M. Compérat JAE, R. Fietkau, G. Gakis,, A.G. van der Heijden (Vice-chair) AL, P. Mariappan,, R.P. Meijer MIM, Y. Neuzillet, V. Panebianco,, M. Rink (Vice-chair) MR, G.N. Thalmann, Patient Advocates: J. Redlef SS, Guidelines Associates: M. Kailavasan AM, L.S. Mertens, editors. EAU Guidelines on Muscle-invasive and metastatic bladder cancer. . EAU Annual Congress; 2024; Paris.

11. Stein JP, Lieskovsky G, Cote R, Groshen S, Feng AC, Boyd S, Skinner E, Bochner B, Thangathurai D, Mikhail M, Raghavan D, Skinner DG. Radical cystectomy in the treatment of invasive bladder cancer: long-term results in 1,054 patients. J Clin Oncol. 2001;19(3):666-675.

12. Alfred Witjes J, Max Bruins H, Carrion A, Cathomas R, Comperat E, Efstathiou JA, Fietkau R, Gakis G, Lorch A, Martini A, Mertens LS, Meijer RP, Milowsky MI, Neuzillet Y, Panebianco V, Redlef J, Rink M, Rouanne M, Thalmann GN, Saebjornsen S, Veskimae E, van der Heijden AG. European Association of Urology Guidelines on Muscle-invasive and Metastatic Bladder Cancer: Summary of the 2023 Guidelines. Eur Urol. 2024;85(1):17-31.

13. Yin M, Joshi M, Meijer RP, Glantz M, Holder S, Harvey HA, Kaag M, Fransen van de Putte EE, Horenblas S, Drabick JJ. Neoadjuvant Chemotherapy for Muscle-Invasive Bladder Cancer: A Systematic Review and Two-Step Meta-Analysis. Oncologist. 2016;21(6):708-715.

14. Sherif A, Holmberg L, Rintala E, Mestad O, Nilsson J, Nilsson S, Malmstrom PU, Nordic Urothelial Cancer G. Neoadjuvant cisplatinum based combination chemotherapy in patients with invasive bladder cancer: a combined analysis of two Nordic studies. Eur Urol. 2004;45(3):297-303.

15. Boeri L, Soligo M, Frank I, Boorjian SA, Thompson RH, Tollefson M, Quevedo FJ, Cheville JC, Karnes RJ. Delaying Radical Cystectomy After Neoadjuvant Chemotherapy for Muscle-invasive Bladder Cancer is Associated with Adverse Survival Outcomes. Eur Urol Oncol. 2019;2(4):390-396.

16. Necchi A, Anichini A, Raggi D, Briganti A, Massa S, Luciano R, Colecchia M, Giannatempo P, Mortarini R, Bianchi M, Fare E, Monopoli F, Colombo R, Gallina A, Salonia A, Messina A, Ali SM, Madison R, Ross JS, Chung JH, Salvioni R, Mariani L, Montorsi F. Pembrolizumab as Neoadjuvant Therapy Before Radical Cystectomy in Patients With Muscle-Invasive Urothelial Bladder Carcinoma (PURE-01): An Open-Label, Single-Arm, Phase II Study. J Clin Oncol. 2018;36(34):3353-3360.

17. Advanced Bladder Cancer Meta-analysis Collaborators G. Adjuvant Chemotherapy for Muscle-invasive Bladder Cancer: A Systematic Review and Meta-analysis of

Individual Participant Data from Randomised Controlled Trials. Eur Urol. 2022;81(1):50-61.

18. Massari F, Ciccarese C, Santoni M, Iacovelli R, Mazzucchelli R, Piva F, Scarpelli M, Berardi R, Tortora G, Lopez-Beltran A, Cheng L, Montironi R. Metabolic phenotype of bladder cancer. Cancer Treat Rev. 2016;45:46-57.

19. Parikh RB, Feld EK, Galsky MD, Adamson BJ, Cohen AB, Baxi SS, Boursi SB, Christodouleas JP, Vaughn DJ, Meropol NJ, Mamtani R. First-line immune checkpoint inhibitor use in cisplatin-eligible patients with advanced urothelial carcinoma: a secular trend analysis. Future Oncol. 2020;16(2):4341-4345.

20. Gonzalez-Rodriguez E, Rodriguez-Abreu D, Spanish Group for Cancer I-B. Immune Checkpoint Inhibitors: Review and Management of Endocrine Adverse Events. Oncologist. 2016;21(7):804-816.

21. Kamali AN, Bautista JM, Eisenhut M, Hamedifar H. Immune checkpoints and cancer immunotherapies: insights into newly potential receptors and ligands. Ther Adv Vaccines Immunother. 2023;11:25151355231192043.

22. Huang PW, Chang JW. Immune checkpoint inhibitors win the 2018 Nobel Prize. Biomed J. 2019;42(5):299-306.

23. O'Neill RE, Cao X. Co-stimulatory and co-inhibitory pathways in cancer immunotherapy. Adv Cancer Res. 2019;143:145-194.

24. Schutz F, Stefanovic S, Mayer L, von Au A, Domschke C, Sohn C. PD-1/PD-L1 Pathway in Breast Cancer. Oncol Res Treat. 2017;40(5):294-297.

25. Tang Q, Chen Y, Li X, Long S, Shi Y, Yu Y, Wu W, Han L, Wang S. The role of PD-1/PD-L1 and application of immune-checkpoint inhibitors in human cancers. Front Immunol. 2022;13:964442.

26. ESMO: First PD-1 checkpoint inhibitor to receive agency approval [Internet]. 2014 [Cited 2024 Dec 4]. Available from: https://www.esmo.org/oncology-news/archive/fda-approves-pembrolizumab-for-advanced-melanoma.

27. Shiravand Y, Khodadadi F, Kashani SMA, Hosseini-Fard SR, Hosseini S, Sadeghirad H, Ladwa R, O'Byrne K, Kulasinghe A. Immune Checkpoint Inhibitors in Cancer Therapy. Curr Oncol. 2022;29(5):3044-3060.

28. Hargadon KM, Johnson CE, Williams CJ. Immune checkpoint blockade therapy for cancer: An overview of FDA-approved immune checkpoint inhibitors. Int Immunopharmacol. 2018;62:29-39.

29. Suzman DL, Agrawal S, Ning YM, Maher VE, Fernandes LL, Karuri S, Tang S, Sridhara R, Schroeder J, Goldberg KB, Ibrahim A, McKee AE, Pazdur R, Beaver JA. FDA Approval Summary: Atezolizumab or Pembrolizumab for the Treatment of Patients with Advanced Urothelial Carcinoma Ineligible for Cisplatin-Containing Chemotherapy. Oncologist. 2019;24(4):563-569.

30. Balar AV, Castellano D, O'Donnell PH, Grivas P, Vuky J, Powles T, Plimack ER, Hahn NM, de Wit R, Pang L, Savage MJ, Perini RF, Keefe SM, Bajorin D, Bellmunt J. First-line pembrolizumab in cisplatin-ineligible patients with locally advanced and unresectable or metastatic urothelial cancer (KEYNOTE-052): a multicentre, single-arm, phase 2 study. Lancet Oncol. 2017;18(11):1483-1492.

31. Rosenberg JE, Hoffman-Censits J, Powles T, van der Heijden MS, Balar AV, Necchi A, Dawson N, O'Donnell PH, Balmanoukian A, Loriot Y, Srinivas S, Retz MM, Grivas P, Joseph RW, Galsky MD, Fleming MT, Petrylak DP, Perez-Gracia JL, Burris HA, Castellano D, Canil C, Bellmunt J, Bajorin D, Nickles D, Bourgon R, Frampton GM, Cui N, Mariathasan S, Abidoye O, Fine GD, Dreicer R. Atezolizumab in patients with locally advanced and metastatic urothelial carcinoma who have progressed following treatment with platinum-based chemotherapy: a single-arm, multicentre, phase 2 trial. Lancet. 2016;387(10031):1909-1920.

32. Bellmunt J, de Wit R, Vaughn DJ, Fradet Y, Lee JL, Fong L, Vogelzang NJ, Climent MA, Petrylak DP, Choueiri TK, Necchi A, Gerritsen W, Gurney H, Quinn DI, Culine S, Sternberg CN, Mai Y, Poehlein CH, Perini RF, Bajorin DF, Investigators K-. Pembrolizumab as Second-Line Therapy for Advanced Urothelial Carcinoma. N Engl J Med. 2017;376(11):1015-1026.

33. Powles T, Park SH, Voog E, Caserta C, Valderrama BP, Gurney H, Kalofonos H, Radulovic S, Demey W, Ullen A, Loriot Y, Sridhar SS, Tsuchiya N, Kopyltsov E,

Sternberg CN, Bellmunt J, Aragon-Ching JB, Petrylak DP, Laliberte RJ, Huang B, Costa N, Blake-Haskins JA, Grivas P. Plain language summary of results from the JAVELIN Bladder 100 study: avelumab maintenance treatment for advanced urothelial cancer. Future Oncol. 2022;18(19):2361-2371.

34. Bajorin DF, Witjes JA, Gschwend JE, Schenker M, Valderrama BP, Tomita Y, Bamias A, Lebret T, Shariat SF, Park SH, Ye D, Agerbaek M, Enting D, McDermott R, Gajate P, Peer A, Milowsky MI, Nosov A, Neif Antonio J, Jr., Tupikowski K, Toms L, Fischer BS, Qureshi A, Collette S, Unsal-Kacmaz K, Broughton E, Zardavas D, Koon HB, Galsky MD. Adjuvant Nivolumab versus Placebo in Muscle-Invasive Urothelial Carcinoma. N Engl J Med. 2021;384(22):2102-2114.

35. Powles T, Duran I, van der Heijden MS, Loriot Y, Vogelzang NJ, De Giorgi U, Oudard S, Retz MM, Castellano D, Bamias A, Flechon A, Gravis G, Hussain S, Takano T, Leng N, Kadel EE, 3rd, Banchereau R, Hegde PS, Mariathasan S, Cui N, Shen X, Derleth CL, Green MC, Ravaud A. Atezolizumab versus chemotherapy in patients with platinum-treated locally advanced or metastatic urothelial carcinoma (IMvigor211): a multicentre, open-label, phase 3 randomised controlled trial. Lancet. 2018;391(10122):748-757.

36. Galsky MD, Arija JAA, Bamias A, Davis ID, De Santis M, Kikuchi E, Garcia-Del-Muro X, De Giorgi U, Mencinger M, Izumi K, Panni S, Gumus M, Ozguroglu M, Kalebasty AR, Park SH, Alekseev B, Schutz FA, Li JR, Ye D, Vogelzang NJ, Bernhard S, Tayama D, Mariathasan S, Mecke A, Thastrom A, Grande E, Group IMS. Atezolizumab with or without chemotherapy in metastatic urothelial cancer (IMvigor130): a multicentre, randomised, placebo-controlled phase 3 trial. Lancet. 2020;395(10236):1547-1557.

37. Powles T, Csoszi T, Ozguroglu M, Matsubara N, Geczi L, Cheng SY, Fradet Y, Oudard S, Vulsteke C, Morales Barrera R, Flechon A, Gunduz S, Loriot Y, Rodriguez-Vida A, Mamtani R, Yu EY, Nam K, Imai K, Homet Moreno B, Alva A, Investigators K-. Pembrolizumab alone or combined with chemotherapy versus chemotherapy as first-line therapy for advanced urothelial carcinoma (KEYNOTE-361): a randomised, open-label, phase 3 trial. Lancet Oncol. 2021;22(7):931-945.

38. US Drug and Food Administration: FDA limits the use of Tecentriq and Keytruda for some urothelial cancer patients [Internet]. 2018 Available from: https://www.fda.gov/drugs/resources-information-approved-drugs/fda-limits-use-tecentriq-and-keytruda-some-urothelial-cancer-patients.

39. Katkade VB, Sanders KN, Zou KH. Real world data: an opportunity to supplement existing evidence for the use of long-established medicines in health care decision making. J Multidiscip Healthc. 2018;11:295-304.

40. Sherman RE, Anderson SA, Dal Pan GJ, Gray GW, Gross T, Hunter NL, LaVange L, Marinac-Dabic D, Marks PW, Robb MA, Shuren J, Temple R, Woodcock J, Yue LQ, Califf RM. Real-World Evidence - What Is It and What Can It Tell Us? N Engl J Med. 2016;375(23):2293-2297.

41. Jenkins RW, Barbie DA, Flaherty KT. Mechanisms of resistance to immune checkpoint inhibitors. Br J Cancer. 2018;118(1):9-16.

42. Paucek RD, Baltimore D, Li G. The Cellular Immunotherapy Revolution: Arming the Immune System for Precision Therapy. Trends Immunol. 2019;40(4):292-309.

43. Drake CG, Bivalacqua TJ, Hahn NM. Programmed Cell Death Ligand-1 Blockade in Urothelial Bladder Cancer: To Select or Not to Select. J Clin Oncol. 2016;34(26):3115-3116.

44. Sharma P, Retz M, Siefker-Radtke A, Baron A, Necchi A, Bedke J, Plimack ER, Vaena D, Grimm MO, Bracarda S, Arranz JA, Pal S, Ohyama C, Saci A, Qu X, Lambert A, Krishnan S, Azrilevich A, Galsky MD. Nivolumab in metastatic urothelial carcinoma after platinum therapy (CheckMate 275): a multicentre, single-arm, phase 2 trial. Lancet Oncol. 2017;18(3):312-322.

45. Zajac M, Scott M, Ratcliffe M, Scorer P, Barker C, Al-Masri H, Rebelatto MC, Walker J. Concordance among four commercially available, validated programmed cell death ligand-1 assays in urothelial carcinoma. Diagn Pathol. 2019;14(1):99.

46. Paliogiannis P, Lobrano R, Bella MA, Fara A, Uras MG, Pinna MA, Tedde A, Madonia M, Zinellu A, Cossu A. PD-L1 immunohistochemical expression in bladder urothelial cancer with SP263, SP142 and 22C3 antibodies: A comparative study. Ann Diagn Pathol. 2024;69:152267.

47. Aggen DH, Drake CG. Biomarkers for immunotherapy in bladder cancer: a moving target. J Immunother Cancer. 2017;5(1):94.

48. Bai J, Gao Z, Li X, Dong L, Han W, Nie J. Regulation of PD-1/PD-L1 pathway and resistance to PD-1/PD-L1 blockade. Oncotarget. 2017;8(66):110693-110707.

49. Zerdes I, Matikas A, Bergh J, Rassidakis GZ, Foukakis T. Genetic, transcriptional and post-translational regulation of the programmed death protein ligand 1 in cancer: biology and clinical correlations. Oncogene. 2018;37(34):4639-4661.

50. Powles T, van der Heijden MS, Castellano D, Galsky MD, Loriot Y, Petrylak DP, Ogawa O, Park SH, Lee JL, De Giorgi U, Bogemann M, Bamias A, Eigl BJ, Gurney H, Mukherjee SD, Fradet Y, Skoneczna I, Tsiatas M, Novikov A, Suarez C, Fay AP, Duran I, Necchi A, Wildsmith S, He P, Angra N, Gupta AK, Levin W, Bellmunt J, investigators Ds. Durvalumab alone and durvalumab plus tremelimumab versus chemotherapy in previously untreated patients with unresectable, locally advanced or metastatic urothelial carcinoma (DANUBE): a randomised, open-label, multicentre, phase 3 trial. Lancet Oncol. 2020;21(12):1574-1588.

51. Dezutter-Dambuyant C, Durand I, Alberti L, Bendriss-Vermare N, Valladeau-Guilemond J, Duc A, Magron A, Morel AP, Sisirak V, Rodriguez C, Cox D, Olive D, Caux C. A novel regulation of PD-1 ligands on mesenchymal stromal cells through MMP-mediated proteolytic cleavage. Oncoimmunology. 2016;5(3):e1091146.

52. Costantini A, Julie C, Dumenil C, Helias-Rodzewicz Z, Tisserand J, Dumoulin J, Giraud V, Labrune S, Chinet T, Emile JF, Giroux Leprieur E. Predictive role of plasmatic biomarkers in advanced non-small cell lung cancer treated by nivolumab. Oncoimmunology. 2018;7(8):e1452581.

53. Kushlinskii NE, Gershtein ES, Morozov AA, Goryacheva IO, Filipenko ML, Alferov AA, Bezhanova SD, Bazaev VV, Kazantseva IA. Soluble Ligand of the Immune Checkpoint Receptor (sPD-L1) in Blood Serum of Patients with Renal Cell Carcinoma. Bull Exp Biol Med. 2019;166(3):353-357.

54. Wang P, Chen Y, Wang C. Beyond Tumor Mutation Burden: Tumor Neoantigen Burden as a Biomarker for Immunotherapy and Other Types of Therapy. Front Oncol. 2021;11:672677.

55. Lawrence MS, Stojanov P, Mermel CH, Robinson JT, Garraway LA, Golub TR, Meyerson M, Gabriel SB, Lander ES, Getz G. Discovery and saturation analysis of cancer genes across 21 tumour types. Nature. 2014;505(7484):495-501.

56. Sharma P, Callahan MK, Bono P, Kim J, Spiliopoulou P, Calvo E, Pillai RN, Ott PA, de Braud F, Morse M, Le DT, Jaeger D, Chan E, Harbison C, Lin CS, Tschaika M, Azrilevich A, Rosenberg JE. Nivolumab monotherapy in recurrent metastatic urothelial carcinoma (CheckMate 032): a multicentre, open-label, two-stage, multi-arm, phase 1/2 trial. Lancet Oncol. 2016;17(11):1590-1598.

57. Bakaloudi DR, Talukder R, Makrakis D, Diamantopoulos L, Enright T, Leary JB, Patgunarajah U, Thomas VM, Swami U, Agarwal N, Jindal T, Koshkin VS, Brown JR, Barata P, Murgic J, Miletic M, Johnson J, Zakharia Y, Hui G, Drakaki A, Duran I, Buznego LA, Barrera RM, Castaneda DM, Rey-Cardenas M, Castellano D, Nguyen CB, Park JJ, Alva A, McKay RR, Stewart TF, Epstein IB, Bellmunt J, Wright JL, Gupta S, Grivas P, Khaki AR. Association of Tumor Mutational Burden and Microsatellite Instability With Response and Outcomes in Patients With Urothelial Carcinoma Treated With Immune Checkpoint Inhibitor. Clin Genitourin Cancer. 2024;22(6):102198.

58. Warrick JI, Al-Ahmadie H, Berman DM, Black PC, Flaig TW, Hoglund M, Bubendorf L, van der Kwast TH, Cheng L, Members of the IBTCP. International Society of Urological Pathology Consensus Conference on Current Issues in Bladder Cancer. Working Group 4: Molecular Subtypes of Bladder Cancer-Principles of Classification and Emerging Clinical Utility. Am J Surg Pathol. 2024;48(1):e32-e42.

59. Szarvas T, Olah C, Riesz P, Geczi L, Nyirady P. [Molecular subtype classification of urothelial bladder cancer and its clinical relevance]. Orv Hetil. 2019;160(42):1647-1654.

60. Kamoun A, de Reynies A, Allory Y, Sjodahl G, Robertson AG, Seiler R, Hoadley KA, Groeneveld CS, Al-Ahmadie H, Choi W, Castro MAA, Fontugne J, Eriksson

P, Mo Q, Kardos J, Zlotta A, Hartmann A, Dinney CP, Bellmunt J, Powles T, Malats N, Chan KS, Kim WY, McConkey DJ, Black PC, Dyrskjot L, Hoglund M, Lerner SP, Real FX, Radvanyi F, Bladder Cancer Molecular Taxonomy G. A Consensus Molecular Classification of Muscle-invasive Bladder Cancer. Eur Urol. 2020;77(4):420-433.

61. Iacovino ML, Miceli CC, De Felice M, Barone B, Pompella L, Chiancone F, Di Zazzo E, Tirino G, Della Corte CM, Imbimbo C, De Vita F, Crocetto F. Novel Therapeutic Opportunities in Neoadjuvant Setting in Urothelial Cancers: A New Horizon Opened by Molecular Classification and Immune Checkpoint Inhibitors. Int J Mol Sci. 2022;23(3).

62. Robertson AG, Meghani K, Cooley LF, McLaughlin KA, Fall LA, Yu Y, Castro MAA, Groeneveld CS, de Reynies A, Nazarov VI, Tsvetkov VO, Choy B, Raggi D, Marandino L, Montorsi F, Powles T, Necchi A, Meeks JJ. Expression-based subtypes define pathologic response to neoadjuvant immune-checkpoint inhibitors in muscle-invasive bladder cancer. Nat Commun. 2023;14(1):2126.

63. Kim J, Kwiatkowski D, McConkey DJ, Meeks JJ, Freeman SS, Bellmunt J, Getz G, Lerner SP. The Cancer Genome Atlas Expression Subtypes Stratify Response to Checkpoint Inhibition in Advanced Urothelial Cancer and Identify a Subset of Patients with High Survival Probability. Eur Urol. 2019;75(6):961-964.

64. Mariathasan S, Turley SJ, Nickles D, Castiglioni A, Yuen K, Wang Y, Kadel EE, III, Koeppen H, Astarita JL, Cubas R, Jhunjhunwala S, Banchereau R, Yang Y, Guan Y, Chalouni C, Ziai J, Senbabaoglu Y, Santoro S, Sheinson D, Hung J, Giltnane JM, Pierce AA, Mesh K, Lianoglou S, Riegler J, Carano RAD, Eriksson P, Hoglund M, Somarriba L, Halligan DL, van der Heijden MS, Loriot Y, Rosenberg JE, Fong L, Mellman I, Chen DS, Green M, Derleth C, Fine GD, Hegde PS, Bourgon R, Powles T. TGFbeta attenuates tumour response to PD-L1 blockade by contributing to exclusion of T cells. Nature. 2018;554(7693):544-548.

65. Wang L, Saci A, Szabo PM, Chasalow SD, Castillo-Martin M, Domingo-Domenech J, Siefker-Radtke A, Sharma P, Sfakianos JP, Gong Y, Dominguez-Andres A, Oh WK, Mulholland D, Azrilevich A, Hu L, Cordon-Cardo C, Salmon

H, Bhardwaj N, Zhu J, Galsky MD. EMT- and stroma-related gene expression and resistance to PD-1 blockade in urothelial cancer. Nat Commun. 2018;9(1):3503.

66. Abuhelwa AY, Bellmunt J, Kichenadasse G, McKinnon RA, Rowland A, Sorich MJ, Hopkins AM. Enhanced Bellmunt Risk Score for Survival Prediction in Urothelial Carcinoma Treated With Immunotherapy. Clin Genitourin Cancer. 2022;20(2):132-138.

67. Bellmunt J, Choueiri TK, Fougeray R, Schutz FA, Salhi Y, Winquist E, Culine S, von der Maase H, Vaughn DJ, Rosenberg JE. Prognostic factors in patients with advanced transitional cell carcinoma of the urothelial tract experiencing treatment failure with platinum-containing regimens. J Clin Oncol. 2010;28(11):1850-1855.

68. Olah C, Reis H, Hoffmann MJ, Mairinger F, Ting S, Hadaschik B, Krafft U, Grunwald V, Nyirady P, Varadi M, Gyorffy B, Kiss A, Szekely E, Sjodahl G, Szarvas T. Predictive value of molecular subtypes and APOBEC3G for adjuvant chemotherapy in urothelial bladder cancer. Cancer Med. 2023;12(5):5222-5232.

69. Olah C, Hahnen C, Nagy N, Musial J, Varadi M, Nyiro G, Gyorffy B, Hadaschik B, Rawitzer J, Ting S, Sjodahl G, Hoffmann MJ, Reis H, Szarvas T. A quantitative polymerase chain reaction based method for molecular subtype classification of urinary bladder cancer-Stromal gene expressions show higher prognostic values than intrinsic tumor genes. Int J Cancer. 2022;150(5):856-867.

70. Holm S. A Simple Sequentially Rejective Multiple Test Procedure. Scandinavian Journal of Statistics. 1979;6(2):65-70.

71. Benjamini Y, Hochberg Y. Controlling the False Discovery Rate: A Practical and Powerful Approach to Multiple Testing. Journal of the Royal Statistical Society. Series B (Methodological). 1995;57(1):289-300.

72. Kovacs SA, Fekete JT, Gyorffy B. Predictive biomarkers of immunotherapy response with pharmacological applications in solid tumors. Acta Pharmacol Sin. 2023;44(9):1879-1889.

73. Fradet Y, Bellmunt J, Vaughn DJ, Lee JL, Fong L, Vogelzang NJ, Climent MA, Petrylak DP, Choueiri TK, Necchi A, Gerritsen W, Gurney H, Quinn DI, Culine S, Sternberg CN, Nam K, Frenkl TL, Perini RF, de Wit R, Bajorin DF. Randomized

phase III KEYNOTE-045 trial of pembrolizumab versus paclitaxel, docetaxel, or vinflunine in recurrent advanced urothelial cancer: results of >2 years of follow-up. Ann Oncol. 2019;30(6):970-976.

74. Vuky J, Balar AV, Castellano D, O'Donnell PH, Grivas P, Bellmunt J, Powles T, Bajorin D, Hahn NM, Savage MJ, Fang X, Godwin JL, Frenkl TL, Homet Moreno B, de Wit R, Plimack ER. Long-Term Outcomes in KEYNOTE-052: Phase II Study Investigating First-Line Pembrolizumab in Cisplatin-Ineligible Patients With Locally Advanced or Metastatic Urothelial Cancer. J Clin Oncol. 2020;38(23):2658-2666.

75. Vander Velde N, Guerin A, Ionescu-Ittu R, Shi S, Wu EQ, Lin SW, Hsu LI, Saum KU, de Ducla S, Wang J, Li S, Thastrom A, Liu S, Shi L, Leppert JT. Comparative Effectiveness of Non-cisplatin First-line Therapies for Metastatic Urothelial Carcinoma: Phase 2 IMvigor210 Study Versus US Patients Treated in the Veterans Health Administration. Eur Urol Oncol. 2019;2(1):12-20.

76. Tan YY, Papez V, Chang WH, Mueller SH, Denaxas S, Lai AG. Comparing clinical trial population representativeness to real-world populations: an external validity analysis encompassing 43 895 trials and 5 685 738 individuals across 989 unique drugs and 286 conditions in England. Lancet Healthy Longev. 2022;3(10):e674-e689.

77. Kennedy-Martin T, Curtis S, Faries D, Robinson S, Johnston J. A literature review on the representativeness of randomized controlled trial samples and implications for the external validity of trial results. Trials. 2015;16:495.

78. Blonde L, Khunti K, Harris SB, Meizinger C, Skolnik NS. Interpretation and Impact of Real-World Clinical Data for the Practicing Clinician. Adv Ther. 2018;35(11):1763-1774.

79. Yanagisawa T, Mori K, Katayama S, Mostafaei H, Quhal F, Laukhtina E, Rajwa P, Motlagh RS, Aydh A, Konig F, Grossmann NC, Pradere B, Miki J, Kimura T, Egawa S, Shariat SF. Pretreatment clinical and hematologic prognostic factors of metastatic urothelial carcinoma treated with pembrolizumab: a systematic review and meta-analysis. Int J Clin Oncol. 2022;27(1):59-71.

80. Dong F, Shen Y, Gao F, Xu T, Wang X, Zhang X, Zhong S, Zhang M, Chen S, Shen Z. Prognostic value of site-specific metastases and therapeutic roles of surgery for patients with metastatic bladder cancer: a population-based study. Cancer Manag Res. 2017;9:611-626.

81. Tural D, Olmez OF, Sumbul AT, Artac M, Ozhan N, Akar E, Cakar B, Kostek O, Ekenel M, Erman M, Coskun HS, Selcukbiricik F, Keskin O, Turkoz FP, Oruc K, Bayram S, Yilmaz U, Bilgetekin I, Yildiz B, Sendur MAN, Paksoy N, Dirican A, Erdem D, Selam M, Tanriverdi O, Paydas S, Urakci Z, Atag E, Guncan S, Urun Y, Alkan A, Kaya AO, Ozyukseler DT, Taskaynatan H, Yildirim M, Sonmez M, Basoglu T, Gunduz S, Kilickap S. Atezolizumab in Patients with Metastatic Urothelial Carcinoma Who Have Progressed After First-line Chemotherapy: Results of Real-life Experiences. Eur Urol Focus. 2021;7(5):1061-1066.

82. Ruiz-Banobre J, Molina-Diaz A, Fernandez-Calvo O, Fernandez-Nunez N, Medina-Colmenero A, Santome L, Lazaro-Quintela M, Mateos-Gonzalez M, Garcia-Cid N, Lopez-Lopez R, Vazquez S, Anido-Herranz U. Rethinking prognostic factors in locally advanced or metastatic urothelial carcinoma in the immune checkpoint blockade era: a multicenter retrospective study. ESMO Open. 2021;6(2):100090.

83. Park JH, Park I, Kim IH, Hur JY, Hwang I, Kim C, Kim HJ, Maeng CH, Park K, Lee MY, Lee HJ, Jung JY, Keam B, Park SH, Lee JL. Prognostic model in patients with metastatic urothelial carcinoma receiving immune checkpoint inhibitors after platinum failure. Curr Probl Cancer. 2022;46(3):100848.

84. ASCO 2022: Defining “Platinum-Ineligible” Patients with Metastatic Urothelial Cancer (mUC) [Internet] 2022 [Cited: 2024 Dec 4]. Available from: https://www.urotoday.com/conference-highlights/asco-2022/asco-2022-bladder-cancer/137614-asco-2022-defining-platinum-ineligible-patients-with-metastatic-urothelial-cancer-muc.html.

85. Chalker C, Voutsinas JM, Wu QV, Santana-Davila R, Hwang V, Baik CS, Lee S, Barber B, Futran ND, Houlton JJ, Laramore GE, Liao JJ, Parvathaneni U, Martins RG, Eaton KD, Rodriguez CP. Performance status (PS) as a predictor of poor

response to immune checkpoint inhibitors (ICI) in recurrent/metastatic head and neck cancer (RMHNSCC) patients. Cancer Med. 2022;11(22):4104-4111.

86. Kapoor A, Noronha V, Patil VM, Menon N, Joshi A, Abraham G, Prabhash K. Immune checkpoint inhibitors in patients with solid tumors and poor performance status: A prospective data from the real-world settings. Medicine (Baltimore). 2021;100(13):e25115.

87. Wells L, Cerniglia M, Hall S, Jost AC, Britt G. Treatment of Metastatic Disease with Immune Checkpoint Inhibitors Nivolumab and Pembrolizumab: Effect of Performance Status on Clinical Outcomes. J Immunother Precis Oncol. 2022;5(2):37-42.

88. Khaki AR, Li A, Diamantopoulos LN, Miller NJ, Carril-Ajuria L, Castellano D, De Kouchkovsky I, Koshkin V, Park J, Alva A, Bilen MA, Stewart T, Santos V, Agarwal N, Jain J, Zakharia Y, Morales-Barrera R, Devitt M, Nelson A, Hoimes CJ, Shreck E, Gartrell BA, Sankin A, Tripathi A, Zakopoulou R, Bamias A, Rodriguez-Vida A, Drakaki A, Liu S, Kumar V, Lythgoe MP, Pinato DJ, Murgic J, Frobe A, Joshi M, Isaacsson Velho P, Hahn N, Alonso Buznego L, Duran I, Moses M, Barata P, Galsky MD, Sonpavde G, Yu EY, Shankaran V, Lyman GH, Grivas P. A New Prognostic Model in Patients with Advanced Urothelial Carcinoma Treated with First-line Immune Checkpoint Inhibitors. Eur Urol Oncol. 2021;4(3):464-472.

89. Wang L, Shen Y. Imbalance of circulating T-lymphocyte subpopulation in gastric cancer patients correlated with performance status. Clin Lab. 2013;59(3-4):429-433.

90. Jeyakumar G, Kim S, Bumma N, Landry C, Silski C, Suisham S, Dickow B, Heath E, Fontana J, Vaishampayan U. Neutrophil lymphocyte ratio and duration of prior anti-angiogenic therapy as biomarkers in metastatic RCC receiving immune checkpoint inhibitor therapy. J Immunother Cancer. 2017;5(1):82.

91. Park W, Lopes G. Perspectives: Neutrophil-to-lymphocyte Ratio as a Potential Biomarker in Immune Checkpoint Inhibitor for Non-Small-Cell Lung Cancer. Clin Lung Cancer. 2019;20(3):143-147.

92. Zaragoza J, Caille A, Beneton N, Bens G, Christiann F, Maillard H, Machet L. High neutrophil to lymphocyte ratio measured before starting ipilimumab treatment is associated with reduced overall survival in patients with melanoma. Br J Dermatol. 2016;174(1):146-151.

93. Nassar AH, Mouw KW, Jegede O, Shinagare AB, Kim J, Liu CJ, Pomerantz M, Harshman LC, Van Allen EM, Wei XX, McGregor B, Choudhury AD, Preston MA, Dong F, Signoretti S, Lindeman NI, Bellmunt J, Choueiri TK, Sonpavde G, Kwiatkowski DJ. A model combining clinical and genomic factors to predict response to PD-1/PD-L1 blockade in advanced urothelial carcinoma. Br J Cancer. 2020;122(4):555-563.

94. Piccard H, Muschel RJ, Opdenakker G. On the dual roles and polarized phenotypes of neutrophils in tumor development and progression. Crit Rev Oncol Hematol. 2012;82(3):296-309.

95. Restifo NP, Dudley ME, Rosenberg SA. Adoptive immunotherapy for cancer: harnessing the T cell response. Nat Rev Immunol. 2012;12(4):269-281.

96. Kugel CH, 3rd, Douglass SM, Webster MR, Kaur A, Liu Q, Yin X, Weiss SA, Darvishian F, Al-Rohil RN, Ndoye A, Behera R, Alicea GM, Ecker BL, Fane M, Allegrezza MJ, Svoronos N, Kumar V, Wang DY, Somasundaram R, Hu-Lieskovan S, Ozgun A, Herlyn M, Conejo-Garcia JR, Gabrilovich D, Stone EL, Nowicki TS, Sosman J, Rai R, Carlino MS, Long GV, Marais R, Ribas A, Eroglu Z, Davies MA, Schilling B, Schadendorf D, Xu W, Amaravadi RK, Menzies AM, McQuade JL, Johnson DB, Osman I, Weeraratna AT. Age Correlates with Response to Anti-PD1, Reflecting Age-Related Differences in Intratumoral Effector and Regulatory T-Cell Populations. Clin Cancer Res. 2018;24(21):5347-5356.

97. Gupta S, Gollapudi S. CD95-mediated apoptosis in naive, central and effector memory subsets of CD4+ and CD8+ T cells in aged humans. Exp Gerontol. 2008;43(4):266-274.

98. Koch S, Larbi A, Derhovanessian E, Ozcelik D, Naumova E, Pawelec G. Multiparameter flow cytometric analysis of CD4 and CD8 T cell subsets in young and old people. Immun Ageing. 2008;5:6.

99. Lages CS, Lewkowich I, Sproles A, Wills-Karp M, Chougnet C. Partial restoration of T-cell function in aged mice by in vitro blockade of the PD-1/ PD-L1 pathway. Aging Cell. 2010;9(5):785-798.

100. Elias R, Giobbie-Hurder A, McCleary NJ, Ott P, Hodi FS, Rahma O. Efficacy of PD-1 & PD-L1 inhibitors in older adults: a meta-analysis. J Immunother Cancer. 2018;6(1):26.

101. Morozov AV, Karpov VL. Proteasomes and Several Aspects of Their Heterogeneity Relevant to Cancer. Front Oncol. 2019;9:761.

102. Hwang S, Kwon AY, Jeong JY, Kim S, Kang H, Park J, Kim JH, Han OJ, Lim SM, An HJ. Immune gene signatures for predicting durable clinical benefit of anti-PD-1 immunotherapy in patients with non-small cell lung cancer. Sci Rep. 2020;10(1):643.

103. Kalaora S, Lee JS, Barnea E, Levy R, Greenberg P, Alon M, Yagel G, Bar Eli G, Oren R, Peri A, Patkar S, Bitton L, Rosenberg SA, Lotem M, Levin Y, Admon A, Ruppin E, Samuels Y. Immunoproteasome expression is associated with better prognosis and response to checkpoint therapies in melanoma. Nat Commun. 2020;11(1):896.

104. Kumar R, Dhaka B, Sahoo S, Jolly MK, Sabarinathan R. Prognostic association of immunoproteasome expression in solid tumours is governed by the immediate immune environment. Mol Oncol. 2023;17(6):1041-1059.

105. Wang Y, Yan K, Lin J, Liu Y, Wang J, Li X, Li X, Hua Z, Zheng Z, Shi J, Sun S, Bi J. CD8+ T Cell Co-Expressed Genes Correlate With Clinical Phenotype and Microenvironments of Urothelial Cancer. Front Oncol. 2020;10:553399.

106. Wang Y, Yan K, Guo Y, Lu Y, Su H, Li H. IP-score correlated to endogenous tumour antigen peptide processing: A candidate clinical response score algorithm of immune checkpoint inhibitors therapy in multiple cohorts. Front Immunol. 2022;13:1085491.

107. Sonpavde G, Manitz J, Gao C, Tayama D, Kaiser C, Hennessy D, Makari D, Gupta A, Abdullah SE, Niegisch G, Rosenberg JE, Bajorin DF, Grivas P, Apolo AB, Dreicer R, Hahn NM, Galsky MD, Necchi A, Srinivas S, Powles T, Choueiri TK,

Pond GR. Five-Factor Prognostic Model for Survival of Post-Platinum Patients with Metastatic Urothelial Carcinoma Receiving PD-L1 Inhibitors. J Urol. 2020;204(6):1173-1179.

108. Bamias A, Merseburger A, Loriot Y, James N, Choy E, Castellano D, Lopez-Rios F, Calabro F, Kramer M, de Velasco G, Zakopoulou R, Tzannis K, Sternberg CN. New prognostic model in patients with advanced urothelial carcinoma treated with second-line immune checkpoint inhibitors. J Immunother Cancer. 2023;11(1).

109. Incorvaia L, Fanale D, Badalamenti G, Porta C, Olive D, De Luca I, Brando C, Rizzo M, Messina C, Rediti M, Russo A, Bazan V, Iovanna JL. Baseline plasma levels of soluble PD-1, PD-L1, and BTN3A1 predict response to nivolumab treatment in patients with metastatic renal cell carcinoma: a step toward a biomarker for therapeutic decisions. Oncoimmunology. 2020;9(1):1832348.

110. Ji S, Chen H, Yang K, Zhang G, Mao B, Hu Y, Zhang H, Xu J. Peripheral cytokine levels as predictive biomarkers of benefit from immune checkpoint inhibitors in cancer therapy. Biomed Pharmacother. 2020;129:110457.

111. Ugurel S, Schadendorf D, Horny K, Sucker A, Schramm S, Utikal J, Pfohler C, Herbst R, Schilling B, Blank C, Becker JC, Paschen A, Zimmer L, Livingstone E, Horn PA, Rebmann V. Elevated baseline serum PD-1 or PD-L1 predicts poor outcome of PD-1 inhibition therapy in metastatic melanoma. Ann Oncol. 2020;31(1):144-152.

112. Szeles A, Fazekas T, Vancsa S, Varadi M, Kovacs PT, Krafft U, Grunwald V, Hadaschik B, Csizmarik A, Hegyi P, Varadi A, Nyirady P, Szarvas T. Pre-treatment soluble PD-L1 as a predictor of overall survival for immune checkpoint inhibitor therapy: a systematic review and meta-analysis. Cancer Immunol Immunother. 2023;72(5):1061-1073.

113. Chiarucci C, Cannito S, Daffina MG, Amato G, Giacobini G, Cutaia O, Lofiego MF, Fazio C, Giannarelli D, Danielli R, Di Giacomo AM, Coral S, Calabro L, Maio M, Covre A. Circulating Levels of PD-L1 in Mesothelioma Patients from the NIBIT-MESO-1 Study: Correlation with Survival. Cancers (Basel). 2020;12(2).

114. Oh SY, Kim S, Keam B, Kim TM, Kim DW, Heo DS. Soluble PD-L1 is a predictive and prognostic biomarker in advanced cancer patients who receive immune checkpoint blockade treatment. Sci Rep. 2021;11(1):19712.

115. Varadi M, Horvath O, Modos O, Fazekas T, Grunewald CM, Niegisch G, Krafft U, Grunwald V, Hadaschik B, Olah C, Maraz A, Furka A, Szucs M, Nyirady P, Szarvas T. Efficacy of immune checkpoint inhibitor therapy for advanced urothelial carcinoma in real-life clinical practice: results of a multicentric, retrospective study. Sci Rep. 2023;13(1):17378.

116. Krafft U, Olah C, Reis H, Kesch C, Darr C, Grunwald V, Tschirdewahn S, Hadaschik B, Horvath O, Kenessey I, Nyirady P, Varadi M, Modos O, Csizmarik A, Szarvas T. High Serum PD-L1 Levels Are Associated with Poor Survival in Urothelial Cancer Patients Treated with Chemotherapy and Immune Checkpoint Inhibitor Therapy. Cancers (Basel). 2021;13(11).

DOI:10.14753/SE.2025.3157

9. Bibliography of own publications

Publications related to the PhD thesis:

1. **Váradi M**, Horváth O, Módos O, Fazekas T, Grunewald CM, Niegisch G, Krafft U, Grünwald V, Hadaschik B, Olah C, Maráz A, Furka A, Szűcs M, Nyirády P, Szarvas T. Efficacy of immune checkpoint inhibitor therapy for advanced urothelial carcinoma in real-life clinical practice: results of a multicentric, retrospective study. Sci Rep. 2023;13(1):17378. **IF:3.8**

2. Krafft U, Olah C, Reis H, Kesch C, Darr C, Grünwald V, Tschirdewahn S, Hadaschik B, Horvath O, Kenessey I, Nyirady P, **Varadi M**, Modos O, Csizmarik A, Szarvas T. High Serum PD-L1 Levels Are Associated with Poor Survival in Urothelial Cancer Patients Treated with Chemotherapy and Immune Checkpoint Inhibitor Therapy. Cancers (Basel). 2021; 13: 2548. **IF:6.575**

3. Olah C, Hahnen C, Nagy N, Musial J, **Varadi M**, Nyiro G, Gyorffy B, Hadaschik B, Rawitzer J, Ting S, Sjödahl G, Hoffmann MJ, Reis H, Szarvas T. A quantitative polymerase chain reaction based method for molecular subtype classification of urinary bladder cancer-Stromal gene expressions show higher prognostic values than intrinsic tumor genes. Int J Cancer. 2022;150(5):856-867. **IF:6.4**

4. Széles Á, Kovács PT, Csizmarik A, **Váradi M**, Riesz P, Fazekas T, Váncsa S, Hegyi P, Oláh C, Tschirdewahn S, Darr C, Krafft U, Grünwald V, Hadaschik B, Horváth O, Nyirády P, Szarvas T. High Pretreatment Serum PD-L1 Levels Are Associated with Muscle Invasion and Shorter Survival in Upper Tract Urothelial Carcinoma. Biomedicines. 2022;10(10):2560. **IF:4.757**

5. Széles Á, Fazekas T, Váncsa S, **Váradi M**, Kovács PT, Krafft U, Grünwald V, Hadaschik B, Csizmarik A, Hegyi P, Váradi A, Nyirády P, Szarvas T. Pre-treatment soluble PD-L1 as a predictor of overall survival for immune checkpoint inhibitor therapy: a systematic review and meta-analysis. Cancers Immunol Immun. 2023;72(5), 1061–1073. **IF:4.6**

Publications not related to the PhD thesis:

6. Módos O, Bozsaki Á, Nagy C, Habina-Nagy N, Pásztor-Csizmarik A, Keresztes D, C. Oláh, **Váradi M**, Horváth A, Szendrői A, Szűcs M, Keszthelyi A, Nyirády P, Szarvas T. A platinaalapú kemoterápia szerepe a húgyhólyagrák kezelésében – az elmúlt 10 év klinikai tapasztalatainak feldolgozása. Magyar Urológia. 2019;31(2):58-65.

7. Nagy N, Kubik A, Szendrői A, Kenessey I, Módos O, Csizmarik A, **Váradi M**, Keresztes D, Szász MA, Hegyi L, Kovalszky I, Reis H, Hadaschik B, Nyirády P, Szarvas T. Combination of molecular genetic analysis with decision-supporting database in order to identify potentially effective drugs for rare adenocarcinomas of the urinary bladder. Orvosképzés. 2020;95(1):95-.

8. Szarvas T, Hoffmann MJ, Olah C, Szekely E, Kiss A, Hess J, Tschirdewahn S, Hadaschik B, Grotheer V, Nyirady P, Csizmarik A, **Varadi M**, Reis H. MMP-7 Serum and Tissue Levels Are Associated with Poor Survival in Platinum-Treated Bladder Cancer Patients. Diagnostics (Basel). 2020; 11: 48. **IF:3.992**

9. Szarvas T, Csizmarik A, Nagy N, Keresztes D, **Váradi M**, Küronya Z, Riesz P, Nyirády P. Az áttétes kasztrációrezisztens prosztatarák gyógyszer-rezisztenciájának molekuláris vonatkozásai. Orv Hetil. 2020; 161: 813-820. **IF:0.54**

10. Szarvas T, Csizmarik A, **Váradi M**, Fazekas T, Hüttl A, Nyirády P, Hadaschik B, Grünwald V, Tschirdewahn S, Shariat SF, Sevcenco S, Maj-Hes A, Kramer G. The prognostic value of serum MMP-7 levels in prostate cancer patients who received docetaxel, abiraterone, or enzalutamide therapy. Urol Oncol. 2021; 39: 296.e11-296.e19. **IF:2.954**

11. Oláh C, **Váradi M**, Kordáné Horváth O, Nyirády P, Szarvas T. A béltartalom és a vizelet mikrobiom-összetételének onkológiai vonatkozásai. Orv Hetil. 2021;162(15):579-586. **IF:0.707**

12. Szarvas T, Pásztor-Csizmarik A, **Váradi M**, Oláh C, Nyirády P. A prosztatarák és húgyhólyagrák molekuláris hátterének terápiás vonatkozásai. Orvosképzés. 2021;96(3):413-421.

13. Kovács PT, Mayer T, Csizmarik A, **Váradi M**, Oláh C, Széles Á, Tschirdewahn S, Krafft U, Hadaschik B, Nyirády P, Riesz P, Szarvas T. Elevated Pre-Treatment Serum MMP-7 Levels Are Associated with the Presence of Metastasis and Poor Survival in Upper Tract Urothelial Carcinoma. Biomedicines. 2022; 10: 698. **IF:4.757**

14. Kubik A, Pinto Amorim das Virgens I, Szabó A, **Váradi M**, Pásztor-Csizmarik A, Keszthelyi A, Majoros A, Fehérvári P, Hegyi P, Ács N, Nyirády P, SzarvasT. Comprehensive Analysis of the Prognostic Value of Circulating MMP-7 Levels

in Urothelial Carcinoma: A Combined Cohort Analysis, Systematic Review, and Meta-Analysis. Int J Mol Sci. 2023;24(9). **IF:4.9**

15. Módos O, **Váradi M**, Dér B, Keszthelyi A, Szűcs M, Reis H, Nyirády P, Szarvas T. Az urachuscarcinoma aktuális diagnosztikai és kezelési lehetőségei. Orv Hetil. 2023;164(16):602-609. **IF:0.8**

16. Olah C, Reis H, Hoffmann MJ, Mairinger F, Ting S, Hadaschik B, Krafft U, Grünwald V, Nyirady P, **Varadi M**, Győrffy B, Kiss A, Szekely E, Sjödahl G, Szarvas T. Predictive value of molecular subtypes and APOBEC3G for adjuvant chemotherapy in urothelial bladder cancer. Cancer Med. 2023;12:5222-5232. **IF:2.9**

17. **Varadi M**, Nagy N, Reis H, Hadaschik B, Niedworok C, Modos O, Szendroi A, Ablat J, Black PC, Keresztes D, Csizmarik A, Olah C, Gaisa NT, Kiss A, Timar J, Toth E, Csernak E, Gerstner A, Mittal V, Karkampouna S, Kruithof de Julio M, Gyorffy B, Bedics G, Rink M, Fisch M, Nyirady P, Szarvas T. Clinical sequencing identifies potential actionable alterations in a high rate of urachal and primary bladder adenocarcinomas. Cancer Med. 2023;12(7):9041-9054. **IF: 2.9**

18. Csizmarik A, Nagy N, Keresztes D, **Váradi M**, Bracht T, Sitek B, Witzke K, Puhr M, Tornyi I, Lázár J, Takács L, Kramer G, Sevcenco S, Maj-Hes A, Hadaschik B, Nyirády P, Szarvas T. Comparative proteome and serum analysis identified FSCN1 as a marker of abiraterone resistance in castration-resistant prostate cancer. Prostate Cancer Prostatic Disease. 2024;27:451-456. **IF:5.1**

19. Oláh C, Shmorhun O, Klamminger G, Rawitzer J, Sichward L, Hadaschik B, Al-Nader M, Krafft U, Niedworok C, Váradi M, Nyirády P, Kiss A, Székely E, Reis H, Szarvas T. Immunohistochemistry-based molecular subtypes of urothelial carcinoma derive different survival benefit from platinum chemotherapy. Journal of Pathology: Clinical Research. 2025 Jan;11(1):e70017. **IF:3.4**

∑IF: 62.817

DOI:10.14753/SE.2025.3157

10. Acknowledgement

First and foremost, I would like to express my heartfelt gratitude to my supervisor, Prof. Dr. Tibor Szarvas for his trust in me and his unwavering support. I am deeply grateful to him for introducing me to the world of research during my university years and encouraging me to pursue this path. Throughout my PhD research, I could always rely on his guidance, support, and encouragement.

I am profoundly grateful to the Head of the Department of Urology at Semmelweis University, Prof. Dr. Péter Nyirády, for his pivotal role in making this research possible. The resources made available laid a strong foundation for the success of this project.

I am deeply appreciative of all the medical experts in the contributing institutions: National Institute of Oncology; University Hospital Düsseldorf; University Hospital Essen; University Hospital Frankfurt; University of Szeged, Borsod-Abaúj-Zemplén County University Hospital.

Dr. Orsolya Horváth, a clinical oncologist at the Department of Genitourinary Medical Oncology and Clinical Pharmacology National Institute of Oncology has provided constructive support for my work from the very beginning of the research. In addition to valuable data and patient samples, her expertise as a clinical oncologist has greatly contributed to the progress of my work.

I would like to thank Dr. István Kenessey, an expert uro-pathologist, for the thorough yet always efficient evaluation of the collected and processed tumor samples.

I am grateful to the colleagues at the Department of Pathology and Experimental Research at Semmelweis University. I would like to thank Anna Tamási for the precise handling of the collected FFPE tumor blocks. I am deeply appreciative of Krisztina Egedi and Krisztina Császár from the Molecular Diagnostic Division of the Department of Pathology and Experimental Research at Semmelweis University for always being readily available to assist me. I could approach them with my questions, and they consistently provided space for the preparation of various molecular investigations.

I would like to thank Prof. Dr. Csaba Bödör and his colleagues, Dr. Ákos Nagy and Dr. Bence Bátai, for providing me with access to the Nanostring equipment and for teaching me how to use it.

DOI:10.14753/SE.2025.3157

I would like to thank Dr. Zoltán Herold bioinformatician for his help in the proper statistical evaluation of the extensive gene expression data. I am grateful to Dr. Máté Posta for his help in creating the combined model.

I am grateful to all the nurses, medical doctors, and other colleagues at the Department of Urology, Semmelweis University for their support. I would also like to extend my appreciation to all the members of the Uro-oncological research group at the Department of Urology, Semmelweis University. I would like to extend a special thanks to Dr. Anita Pásztor-Csizmarik, who not only provided me with immense help but also shared many enjoyable days in the lab, filled with great atmosphere.

Last but certainly not least, I owe immense gratitude and thanks to my family and friends. I deeply appreciate my parents and my brother for their constant support, standing by me and encouraging me throughout my extended studies. Words cannot express how thankful I am to my husband, who created the opportunity for me to pursue PhD studies, always provided his support, believed in me, and helped me through difficult times. I am also especially grateful to every member of my family for enabling me to continue and successfully complete my research after the birth of my son. Their love and support mean more to me than anything.